Received: 7 February 2022 | Revised: 25 August 2022 | Accepted: 9 September 2022

DOI: 10.1111/bph.15951

RESEARCH ARTICLE

P2X7 receptor activation impairs antitumour activity of natural killer cells

Alberto Baroja-Mazo[1] | Alejandro Peñín-Franch[1] | Fernando Lucas-Ruiz[1] | Carlos de Torre-Minguela[1] | Cristina Alarcón-Vila[1] | Trinidad Hernández-Caselles[1,2] | Pablo Pelegrín[1,2]

[1]Biomedical Research Institute of Murcia (IMIB-Pascual Parrilla), University Clinical Hospital Virgen de la Arrixaca, Murcia, Spain

[2]Department of Biochemistry and Molecular Biology B and Immunology, Faculty of Medicine, University of Murcia, Murcia, Spain

Correspondence
Alberto Baroja-Mazo, Campus de Ciencias de la Salud, Edificio LAIB, Office 4.21, Ctra. Buenavista s/n, 30120, Murcia, Spain.
Email: alberto.baroja@ffis.es

Funding information
We acknowledge PlasticHeal project that has received funding from the European Union's Horizon 2020 research and innovation programme under grant agreement No. 965196. A. B-M. was funded by Fundación Mutua Madrileña (AP171362019), Instituto de Salud Carlos III (PI20/00185) and Fundación Séneca (21655/PDC/21). P. P. was funded by grant PID2020-116709RB-I00 funded by MCIN/AEI/10.13039/501100011033, Fundación Séneca (grants 20859/PI/18, 21081/PDC/19 and 0003/COVI/20), Instituto de Salud Carlos III (grant DTS21/00080) and European Research Council (grant ERC-2019-PoC 899636). F. L-R. has been co-financed by the European Social Fund (ESF) and the Youth European Initiative (YEI) under the Spanish Seneca Foundation (Spain) 21373/PDGI/20, and A. P-F. was funded by MVClnic and Prim. Funding sources provided financial support but had no involvement in study design, collection, analysis and interpretation of data.

Background and purpose: A high number of intratumoural infiltrating natural killer (NK) cells is associated with better survival in several types of cancer, constituting an important first line of defence against tumours. Hypoxia in the core of solid tumours induces cellular stress and ATP release into the extracellular space where it triggers purinergic receptor activation on tumour-associated immune cells. The aim of this study was to assess whether activation of the purinergic receptor P2X7 by extracellular ATP plays a role in the NK cells antitumour activity.

Experimental approach: We carried out in vitro experiments using purified human NK cells triggered through P2X7 by extracellular ATP. NK cell killing activity against the tumour target cells K562 was studied by means of NK cytotoxicity assays. Likewise, we designed a subcutaneous solid tumour in vivo mouse model.

Key results: In this study we found that human NK cells, expressing a functional plasma membrane P2X7, acquired an anergic state after ATP treatment, which impaired their antitumour activity and decreased IFN-γ secretion. This effect was reversed by specific P2X7 antagonists and pretreatment with either IL-2 or IL-15. Furthermore, genetic *P2rx7* knockdown resulted in improved control of tumour size by NK cells. In addition, IL-2 therapy restored the ability of NK cells to diminish the size of tumours.

Conclusions and implications: Our results show that P2X7 activation represents a new mechanism whereby NK cells may lose antitumour effectiveness, opening the possibility of generating modified NK cells lacking P2X7 but with improved antitumour capacity.

KEYWORDS
A438079, ATP, IL-2, natural killer cells, P2X7, tumour environment

Abbreviations: ADAM, a disintegrin and metalloproteinase; ADCC, antibody-dependent cellular cytotoxicity; CAR, chimeric antigen receptor; CFSE, carboxy-fluorescein diacetate succinimidyl ester; MHC, major histocompatibility complex; MMP, matrix metalloproteinase; NK, natural killer; PBMCs, peripheral blood mononuclear cells.

Alejandro Peñín-Franch and Fernando Lucas-Ruiz contributed equally to this work.

1 | INTRODUCTION

The purinergic receptor **P2X7** is a trimeric ion channel gated by extracellular **adenosine 5′-triphosphate** (ATP). P2X7 activation induces different downstream actions in a cell-specific manner, including the release of inflammatory mediators, cell proliferation, cell death or metabolic alterations, therefore playing significant roles in health and disease (Young & Gorecki, 2018). P2X7 is present in different cell types including stem, glial, neural, ocular, bone, dental, exocrine, endothelial, muscle, renal, skin and immune cells (Sluyter, 2017). Monocytes and macrophages are recognized as the cells expressing higher levels of P2X7, being the most studied immune cells for P2X7 activation. Among other functions, triggering P2X7 in M1 polarized macrophages mediates the activation of the **NLRP3** inflammasome with the subsequent release of **IL-1β** and the induction of cell death by pyroptosis (Pelegrin, 2021). However, P2X7 stimulation in M2 polarized macrophages induces the release of anti-inflammatory proteins and does not induce pyroptotic cell death (de Torre-Minguela et al., 2016). Likewise, P2X7 activation in T-lymphocytes is either implicated in the mitogenic stimulation and activation of these cells (Junger, 2011), or associated with ATP-induced cell death (Aswad & Dennert, 2006), affecting the immunosuppressive potential of regulatory T cells (Tregs) (Jacob et al., 2013). This dual action may be related with two states of activation of the P2X7: the cation-selective ion channel or its transition to a large conductance non-selective pore (Adinolfi, Pizzirani, et al., 2005). Although P2X7 is expressed and active in natural killer cells (NK cells) (Gu et al., 2000), little is known of the function of P2X7 in this particular type of immune cell. NK cells are key components of the initial innate immune defence and play a pivotal role in the first line of defence against tumour growth and cancer development (Bryceson & Ljunggren, 2011). Human NK cells can be subdivided into two major subtypes, $CD56^{dim}CD16^{+}$ cytotoxic and $CD56^{bright}CD16^{-}$ immunoregulatory cells. Cytotoxic NK cells directly kill tumour cells without previous stimulation by the cytotoxic effector molecules **perforin 1** and **granzyme B**. To discriminate target tumour cells, NK cells are equipped with a molecular detection system that includes a variety of cell surface activating and inhibitory receptors (Lanier, 2005). Moreover, NK cells also regulate the immune response by secreting different cytokines and chemokines (Vivier et al., 2008). Clinical application of NK cells is an area of intense investigation, especially in haematological malignancies (Gonzalez-Rodriguez et al., 2019), but also in solid tumours such as ovarian cancer, hepatocellular carcinoma or melanoma (Ingram et al., 2021). However, the functional activity of NK cells in the tumour micro-environment is suppressed, and understanding how this micro-environment controls NK cell antitumour activity is critical to develop robust tumour immunotherapy (Ge et al., 2020). In the hypoxic environment of solid tumours, extracellular ATP is elevated (higher than 700 μM) for extended periods of time (Pellegatti et al., 2008) and signals through P2X7 activation in both tumour and tumour-associated immune cells.

Therefore, the aim of the present study was to investigate the effect of extracellular ATP signalling in NK cells, and how P2X7 activation could influence the antitumour activity of these cells in an ATP-rich environment such as that found in solid tumours.

What is already known

- NK cells are the first line of defence against tumours
- Extracellular ATP concentration is elevated in the core of solid tumours

What does this study add

- Extracellular ATP signalling through P2X7 receptor inhibits the antitumour activity of NK cells
- This effect is effectively reversed by IL-2/IL-15 pretreatment of NK cells

What is the clinical significance?

- P2X7 activation in NK cells emerges as a novel mechanism of tumour evasion
- This study paves the way for developing NK cells lacking P2X7 with enhanced antitumour capacity

2 | METHODS

2.1 | Cells and antibodies

Human MHC-I negative erythroblastoid K562 (CCL-243), mouse melanoma B16-F10 (CRL-6322) and mouse mastocytoma FcR^{+} P815 (TIB-64) cell lines were from ATCC. Mouse lymphoma YAC-1 cell were kindly provided by Dr. Detlef Schuppan (Institute of Translational Immunology and Research Center for Immunotherapy, University Medical Center Mainz, Mainz, Germany). HEK293T cells (CRL-11268; ATCC) stably expressing human *P2X7* were previously established in our lab.

Mouse monoclonal anti-human P2X7 clone L4 was a gift of Dr. Koch-Nolte, whereas rabbit polyclonal anti-P2X7 against intracellular epitope was from Alomone Labs. Anti-human Lineage cocktail 3 (CD3/CD19/CD20/CD14)-FITC, CD3-FITC, CD19-FITC, CD16-APCH7, CD14-APCH7, CD62L-PE and CD107a-APC, propidium iodide (PI) as well as GolgiStop (containing monensin) were provided by BD Biosciences; CD56-PECy7 and Ghost Dye Red780 were from Tonbo Biosciences; carboxy-fluorescein diacetate succinimidyl ester (CFSE), YO-PRO-1, Fura-2-AM, anti-mouse CD45-PerCPCy5.5, CD3-FITC, CD8-APC and NKp46-APC, anti-human NKG2D (clone 1D11), anti-NKp46 (clone 6E2) and anti-2B4 (clone C1,7), mouse-IgG

isotype control or fluorescent conjugated secondary anti-mouse or anti-rabbit IgG antibodies were from ThermoFisher; Ultra-LEAF™ Purified anti-mouse NK1.1 was from Biolegend; inVivoMab anti-mouse CD8β (Lyt3.2) was from BioXcell; anti-CD16 (clone KD1) was kindly provided by Dr. A. Moretta (Milan, Italy) and Dr. M. López-Botet (Barcelona, Spain), anti-CD2 (clone TS2/18) and anti-CD18 (clone TS1/18) were a gift from Dr. F. Sánchez-Madrid (Hospital de la Princesa, Madrid, Spain). Anti-CD11a (clone RK1B4) was obtained in our lab. The latter four mAb were used as hybridoma culture supernatant.

2.2 | Materials

ATP, **A438079**, BAPTA-AM, TMI-I (WAY-171318) and **marimastat** were from Sigma-Aldrich. **Caspase 3** inhibitor I and pan-caspase inhibitor (Z-VAD-FMK) were from Merck Millipore. Recombinant human **IL-15**, **IL-12** and **IL-21** were supplied by PeProtech, whereas **IL-2** (Proleukin®) was from Novartis and **IL-18** from Invivogen.

2.3 | Mice

All experimental protocols for animal handling were refined and approved by the Animal Health Service of the General Directorate of Fishing and Farming of the Council of Murcia (Servicio de Sanidad Animal, Dirección General de Ganadería y Pesca, Consejería de Agricultura y Agua Región de Murcia, reference A1320140201). Welfare-related assessments, measurements and interventions were carried out before, during and after experiments. Animal studies are reported in compliance with the ARRIVE 2.0 guidelines (Percie du Sert et al., 2020) and with the recommendations made by the *British Journal of Pharmacology* (Lilley et al., 2020). C57BL/6 mice (WT, wild-type) were purchased from Charles River Laboratories and P2X7 null mice ($P2X7^{-/-}$,B6N-P2rx7tm1d(EUCOMM)Wtsi/Ieg) were generated by Prof. Annette Nicke as previously described (Kaczmarek-Hajek et al., 2018). For all experiments, female mice between 8 and 10 weeks of age were used. Mice were randomly assigned to each group, and 3–5 mice were bred per cage with a 12:12-hr light–dark cycle and used in accordance with the Hospital Clínico Universitario Virgen Arrixaca animal experimentation guidelines, and Spanish national (Royal Decree 1201/2005 and Law 32/2007) and EU (86/609/EEC and 2010/63/EU) legislation.

2.4 | In vivo model of subcutaneous solid tumour

B16-F10 mouse melanoma cell line (ATCC CRL-6475), largely used to study subcutaneous solid tumour development, was grown in DMEM high glucose medium with 10% fetal bovine serum (FBS) and harvested in the logarithmic growth phase. B16-F10 cells (10^6 in 150-μl sterile phosphate buffer saline [PBS]) were injected subcutaneously on the mice back under **isoflurane** anaesthesia and tumour development was followed daily. Mouse eating, drinking, moving and the area operated on was monitored daily. Mice were killed by exposure to CO_2 followed by cervical dislocation 10 days later, and the tumour was excised, weighed, sized and fixed for immunohistochemistry. After killing and tumour extraction, samples were treated with coding numbers for blinding the protocol to avoid subjectivity in the quantification of the different studied parameters. Tumour volume (V) was calculated using the equation: $V = 4/3 \cdot \pi \cdot a \cdot b \cdot c$, being '$a$' half of the length, '$b$' half of the width and 'c' half of the thickness. For $CD8^+$ T cell depletion, all mice received 100 μg of anti-CD8b antibody (clone 53–5.8) intraperitoneally (i.p.) on days −3, 0 and +7. Where indicated, mice were treated i.p. with 5000 U of recombinant human IL-2 daily for 5 days or with 100 μg of anti-NK1.1 (clone PK136) on days −3, 0 and +7.

2.5 | Tumour immunohistochemistry

An indirect ABC immunohistochemical procedure was performed to identify the NK cell infiltrate. Briefly, 3-μm-thick sections of formalin fixed and paraffin embedded tumour samples were analysed by using a specific commercial kit (Vector Impress) following the manufacturer's recommendations. After deparaffination and rehydration, tumour sections underwent a heat-induced demasking antigen procedure (Dako PT-Link) followed by the blocking of endogenous peroxidase and nonspecific background. Tumour sections were then incubated overnight with the primary rabbit polyclonal anti-NKp46 antibody (clone PA5–79720), at 1/500 dilution, followed by incubation with the secondary goat anti-rabbit labelled polymer (Vector Laboratories). Immunoreaction was revealed using 3–3′-diaminobencicine (DAB) (Vector Laboratories) and counterstained with haematoxylin. Positive reaction was identified as a dark-brown membrane patterned precipitate.

2.6 | Cell culture and NK cell isolation

Cell lines and primary lymphocytes were cultured in RPMI medium (DMEM:F12 [1:1] for HEK293T cells) supplemented with 2 mM of L-glutamine and 10% FBS. Peripheral blood mononuclear cells were isolated from fresh blood from healthy volunteers and collected at the Hospital Clínico Universitario Virgen de la Arrixaca (Murcia) upon informed consent. Each separate experiment was performed with cells from a single source. Human NK cells and monocytes were isolated from peripheral blood mononuclear cells (PBMCs) by means of Magnisort Human NK Cell Enrichment Kit (Invitrogen) and EasySep Human Monocyte Enrichment Kit without CD16 Depletion (StemCell Technologies), respectively. Mouse NK cells were isolated from splenocytes by means of MojoSort Mouse NK cell Isolation Kit (Biolegend). Purity of Human NK cells was ≥95% (Figure S1a) and ≥80% for monocytes. After purification, NK cells were incubated with or without the specific P2X7 antagonist A438079 for 10 min and, then, incubated with 3-mM ATP for

30 min. Next, cells were washed, resuspended in medium and used in the different experiments. Other compounds, including metalloprotease or caspase inhibitors, were added before and during ATP treatment. Where indicated, NK cells were incubated in electrophysiological (Et) buffer (147-mM NaCl, 10-mM Hepes, 13-mM D-glucose, 2-mM KCl, 2-mM $CaCl_2$ and 1-mM $MgCl_2$; pH 7.4) (Barbera-Cremades et al., 2012).

The NK target cells K562, YAC-1 and P815 were stained with 5-μM CFSE for 15 min before using in the cytotoxicity assay.

2.7 | Flow cytometry

Cells were stained with fluorescent conjugated antibodies against several surface markers. Human NK cells were defined as Lineage$^-$CD56$^+$CD16$^{+/-}$, and mouse NK cells were selected as CD45$^+$CD3$^-$NKp46$^+$.

For unlabelled primary antibody detection (P2X7 clone L4, **CD11a**, **CD2**, **CD18**, NKG2D, 2B4 or NKp46), cells were first incubated with the primary antibody and, then, washed and stained with a PE or Alexa Fluor 647 conjugated secondary anti-mouse-IgG antibody.

For granzyme B, perforin 1 and **IFN-γ** intracellular staining, cells were incubated with the antibody after fixation and permeabilization with Foxp3/Transcription Factor Staining Buffer Kit (Tonbo Biosciences) as indicated by the manufacturer.

After staining, the cells were subjected to flow cytometry analysis in a BD FACSCanto flow cytometer and FACSDiva software (BD Biosciences) by gating for singlets based on the forward scatter (FSC-A, FSC-H) and side scatter (SSC-A) parameters. NK cell viability was detected by Ghost Dye™ Red 780 (Tonbo Biosciences) staining for 30 min. Data were analysed by FCS Express 5 software (DeNovo Software).

2.8 | Immunofluorescence microscopy

Purified monocytes and NK cells (5×10^4 cells per coverslip) were seeded on poly-L-lysine coated coverslips. After 4 h at 37°C, the cells were washed twice with PBS and then fixed with 4% paraformaldehyde for 15 min at room temperature. Coverslips were washed six times with cold PBS and incubated with blocking/permeabilization solution (10% mouse serum, 0.2% Triton X-100 [Sigma] in PBS) for 1 h at room temperature. After this step, cells were incubated overnight with the anti-P2X7 rabbit polyclonal primary antibody (1:100 dilution) at 4°C. Then, cells were washed with PBS and incubated with AlexaFluor 488 donkey anti-rabbit IgG secondary antibody (1:800 dilution) for 1 h at room temperature, rinsed in PBS and finally incubated for 10 min with **DAPI** (1 μg·ml^{-1}). All coverslips were mounted on slides with Fluorescence mounting solution (DAKO). Images were acquired using a Nikon Eclipse Ti microscope equipped with ×40 S Plan Fluor objective (numerical aperture, 0.6) and 60×/0.60 S Plan Fluor objective and a digital Sight DS-QiMc camera (Nikon, Tokio, Japan) with a Z optical spacing of 0.4 μm and 387-/447-nm, 472-/520-nm filter sets (Semrock). Maximum-intensity projection of images was achieved with NIS-Elements AR software (Nikon) and ImageJ software (US National Institutes of Health).

2.9 | NK cell cytotoxicity assay

Human or mouse NK cells (5×10^4 cells) were cocultured in round-bottom 96-well plates with CFSE stained K562 or YAC-1 target cells, respectively, at 1:1, 1:2, 1:4 and 1:8 effector/target (E/T) ratios. Cells were incubated at 37°C, 5% CO_2 for 2 h. Then, 3-μg·ml^{-1} GolgiStop and anti-CD107a-APC were added to the cells and incubated for two additional hours. Finally, NK cell degranulation was analysed by measuring the membrane expression of CD107a by flow cytometry. Target cell killing was detected in the presence of PI.

2.10 | NK-K562 conjugation assay

Purified human NK cells were stained with Vybrant™ DID for 10 min at 37°C and then treated with ATP and P2X7 antagonists as stated in cell culture section. After that, Vybrant™ DID stained NK cells (5×10^4 cells per well) were cocultured with CFSE stained K562 cells at 1:1, 1:2, 1:4 and 1:8 target: effector ratios in round-bottom 96-well plates. Plates were centrifuged 800 rpm for 2 min without brake, incubated at 37°C, 5% CO_2 for 20 min, and effector/target conjugation was stopped on ice. Cells were directly subjected to flow cytometry analysis to detect Vybrant™ DID$^+$ CFSE$^+$ NK-K562 conjugates.

2.11 | NK cell proliferation assay

Isolated human NK cells (1×10^4 cells per well) were incubated in flat-bottom 96-well plates in the presence of 200-U·ml^{-1} IL-2 or 25-ng·ml^{-1} IL-15 and 50-ng·ml^{-1} IL-21 for 5 days and cell proliferation was determined using the colorimetric Cell Proliferation ELISA BrdU (Roche) following manufacturer's instructions.

2.12 | YO-PRO-1 uptake

Dye uptake was analysed using a Synergy Mx plate reader (BioTek). The 10^5 human monocytes or NK cells were plated in 96-well black clear bottom plates previously coated with poly-L-Lysine for 30 min. Then, YO-PRO-1 solution was added to reach 2-μM final concentration. Fluorescence due to YO-PRO-1 bound DNA was measured at 485/515-nm excitation/emission wavelength for 1–2 h at intervals of 30 s before and during incubation at 37°C with ATP (3 mM). Relative fluorescence units (RFU) are represented over time.

2.13 | Intracellular calcium assay

Similar to YO-PRO experiments, 10^5 human monocytes or NK cells were plated in 96-well black clear bottom plates and incubated with 0.02% pluronic acid supplemented 4-μM Fura-2-AM dye, at 37°C for 40 min in loading buffer (136-mM NaCl, 1.8-mM KCl, 1.2-mM KH_2PO_4, 5-mM $NaHCO_3$, 1.2-mM $MgSO_4$, 20-mM HEPES, 5.5-mM D-glucose and 1-mM ethyleneglycol-bis(β-aminoethyl)-N,N,N′,N′-tetra-acetic acid (EGTA)). At the end of the incubation, Fura-2-AM was removed and replaced with Et buffer. Fluorescence was recorded by an automatic fluorescence plate reader (Synergy Mx; BioTek) for 200 s at 4-s intervals at 340/380-nm excitation couple and 510-nm emission wavelength. ATP (3 mM) was automatically injected into the wells after 20 s of stabilization. Intracellular calcium (Ca^{2+}) level was calculated as the ratio of the emission intensities at 340 and 380 nm, and the value was normalized to the fluorescence at time 0 ($F/F0$).

2.14 | Quantitative RT-PCR

Total RNA was extracted using RNAqueous Micro Kit (Invitrogen), followed by reverse transcription. Quantitative PCR was performed using SYBR Premix ExTaq (Takara). P2X7 specific primers were purchased from Sigma-Aldrich (H_P2RX7_1; KiCqStart® Primers. Forward Human 1 P2RX7: TGTCGCTCCCATATTTATCC; Reverse Human 1 P2RX7: TACTTTAATGTCGGCTTTGG). The samples were run in duplicate, and the relative gene expression levels were calculated using the $2^{-\Delta Ct}$ method (Livak & Schmittgen, 2001), normalizing to 18SRNA.

2.15 | Reverse antibody-dependent cell-mediated cytotoxicity (ADCC) assay

CFSE stained P815 target cells (2.5×10^4) were incubated in round-bottom 96-well plates with variable amounts of human NK cells at 1:2, 1:1 and 1:0.5 target: effector ratios. Cells were incubated at 37°C, 5% CO_2 during 4 h in the presence of 2 μg·ml^{-1} anti-NKp46 (clone 6E2), anti-CD16 (clone KD1) or mouse-IgG isotype control. Cells were analysed by flow cytometry in the presence of PI to detect P815 cell death ($CFSE^+PI^+$ double positive cells).

2.16 | IFN-γ stimulation assay

IFN-γ production was stimulated in human NK cells through three different approaches. First, 5×10^4 human NK cells were cocultured with 2.5×10^4 CFSE stained K562 target cells in round-bottom 96-well plates during 4 h in the presence of 3-μg·ml^{-1} GolgiStop. Then, cells were intracellularly stained with PE-conjugated anti-human IFN-γ antibodies and $CFSE^-$IFN-γ^+ NK cells were detected by flow cytometry. Likewise, 5×10^4 NK cells were cultured with 10-ng·ml^{-1} **phorbol 12-myristate 13-acetate** (PMA) and 500-ng·ml^{-1} ionomycin for 6 h and then IFN-γ expressing cells were detected by flow cytometry. On the other hand, 5×10^4 NK cells were incubated for 16 h in the presence of 200-U·ml^{-1} IL-2 and 20-ng·ml^{-1} IL-12 and then supernatants were collected and assayed for IFN-γ release by a specific ELISA (Invitrogen).

2.17 | Data and statistical analysis

The experimental design and analysis comply with the recommendations and requirements of the *British Journal of Pharmacology* (Curtis et al., 2018). The immune-related procedures used comply with the recommendations made by the *British Journal of Pharmacology* (Alexander et al., 2018). Statistical tests were performed using GraphPad Prism 8.0.2 software (GraphPad Software Inc.). The results are represented as the mean ± SD. All group size was at least $n = 5$ for in vivo and in vitro experiments. The statistical calculations were performed by one-way ANOVA followed by Bonferroni's post hoc tests for multiple comparisons if F reached $P < 0.05$ and there was no significant variance inhomogeneity. Logarithmic transformation of some results was used to avoid unwanted sources of variation. Student's t test was used for comparing two groups. For all comparisons, $P < 0.05$ was accepted to indicate a statistically significant difference. The cells used for each single experiment came from a different donor, and each experiment was conducted in duplicates. For mice experiments, the minimum number of mice necessary to obtain statistically significant differences among groups was used ($n \geq 5$). Values from a single mouse are represented as a dot in its respective figure.

2.18 | Nomenclature of targets and ligands

Key protein targets and ligands in this article are hyperlinked to corresponding entries in http://www.guidetopharmacology.org and are permanently archived in the Concise Guide to PHARMACOLOGY 2021/22 (Alexander et al., 2021b).

3 | RESULTS

3.1 | Human NK cells express a functional P2X7

Purified human peripheral blood **CD56**$^+$ NK cells stained weakly positive for P2X7 surface expression as determined by flow cytometry, compared with monocytes (Figure 1a). P2X7 expression was confirmed both by quantitative PCR (Figure 1b) and immunofluorescence microscopy (Figure S1b), where P2X7 staining was principally intracellular in NK cells, as reported before (Gu et al., 2000). ATP treatment of human NK cells induced intracellular Ca^{2+} increase and YO-PRO-1 uptake that was blocked with the specific P2X7 antagonist A438079 (Figure 1c,d). These results are in agreement with previous studies (Gu et al., 2000) and confirm a functional expression of P2X7 in NK cells,

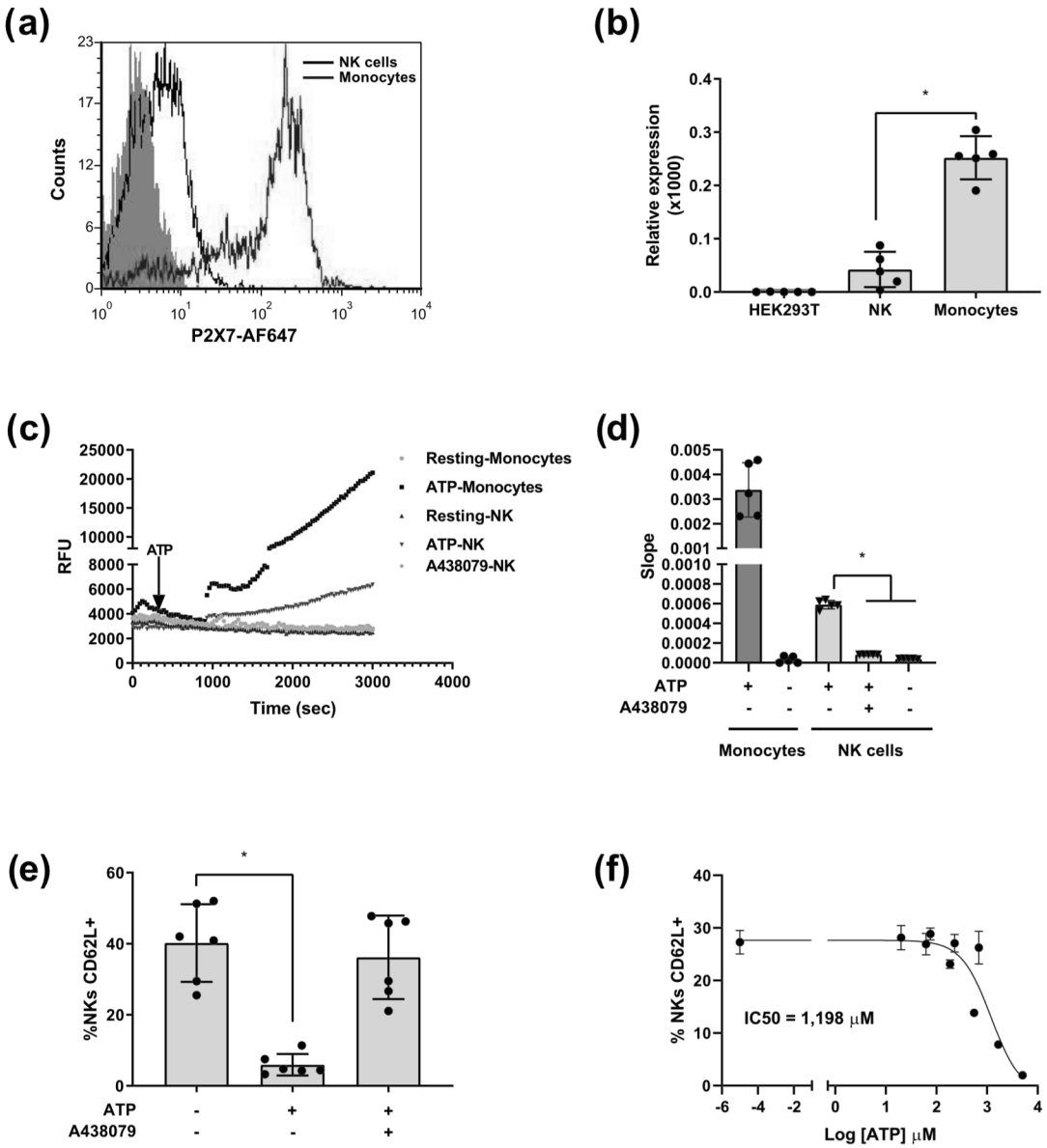

FIGURE 1 Human natural killer (NK) cells express a functional P2X7. (a) P2X7 expression on human NK cells (black line) and monocytes (red line) as measured by flow cytometry in peripheral blood mononuclear cells (PBMCs). FcR expressed on PBMCs were first blocked and then cells were stained using anti-human P2X7 (clone L4) followed by Alexa Fluor 647 conjugated anti-mouse IgG secondary antibody. Afterward, cells were stained using a combination of fluorescent antibodies to detect NK cells (CD3-CD19-CD14-CD56+) and monocytes (CD3-CD19-CD56-CD14+). Filled histogram represents mouse IgG isotype control signal. Representative histograms are shown from five independent experiments. (b) Relative expression of *P2X7* in isolated human NK cells and monocytes as determined by qPCR. HEK293T cells were used as negative control. n = 5. (c) Kinetics of Yo-Pro uptake expressed as relative fluorescent units (RFU) in isolated NK cells and monocytes after the activation with 3-mM ATP in the presence or absence of 50-μM A438079. Representative kinetic graph is shown from six independent experiments. (d) Intracellular Ca^{+2} increase expressed as the slope of the exponential Fura-2-AM signal recorded over time in isolated human NK cells and monocytes after the addition of 3-mM ATP in the presence or absence of 50-μM A438079. n = 5. (e) Frequency of isolated human NK cells expressing CD62L after activation with 3-mM ATP for 30 min in the presence or absence of 50-μM A438079, as measured by flow cytometry. n = 6. (f) Dose–response curve for CD62L shedding induced by ATP on isolated human NK cells. n = 5. Results are presented as the mean ± SD; *$P \leq 0.05$ unpaired Student's *t* test (d) or one-way ANOVA followed by Bonferroni test (b, d and e).

with unknown function in this cell type. ATP treatment of NK cells also resulted in the shedding of the leukocyte adhesion molecule L-selectin (CD62L) (Figure 1e), another functional characteristic of P2X7 activation described in lymphocytes (Jamieson et al., 1996). The shedding of CD62L also occurred in NK cells stimulated in a whole blood assay (Figure S1c). Moreover, only high concentrations of ATP [IC_{50} = 1.2 mM, in the affinity range of P2X7 (Dou et al., 2018)] induced CD62L shedding (Figure 1f).

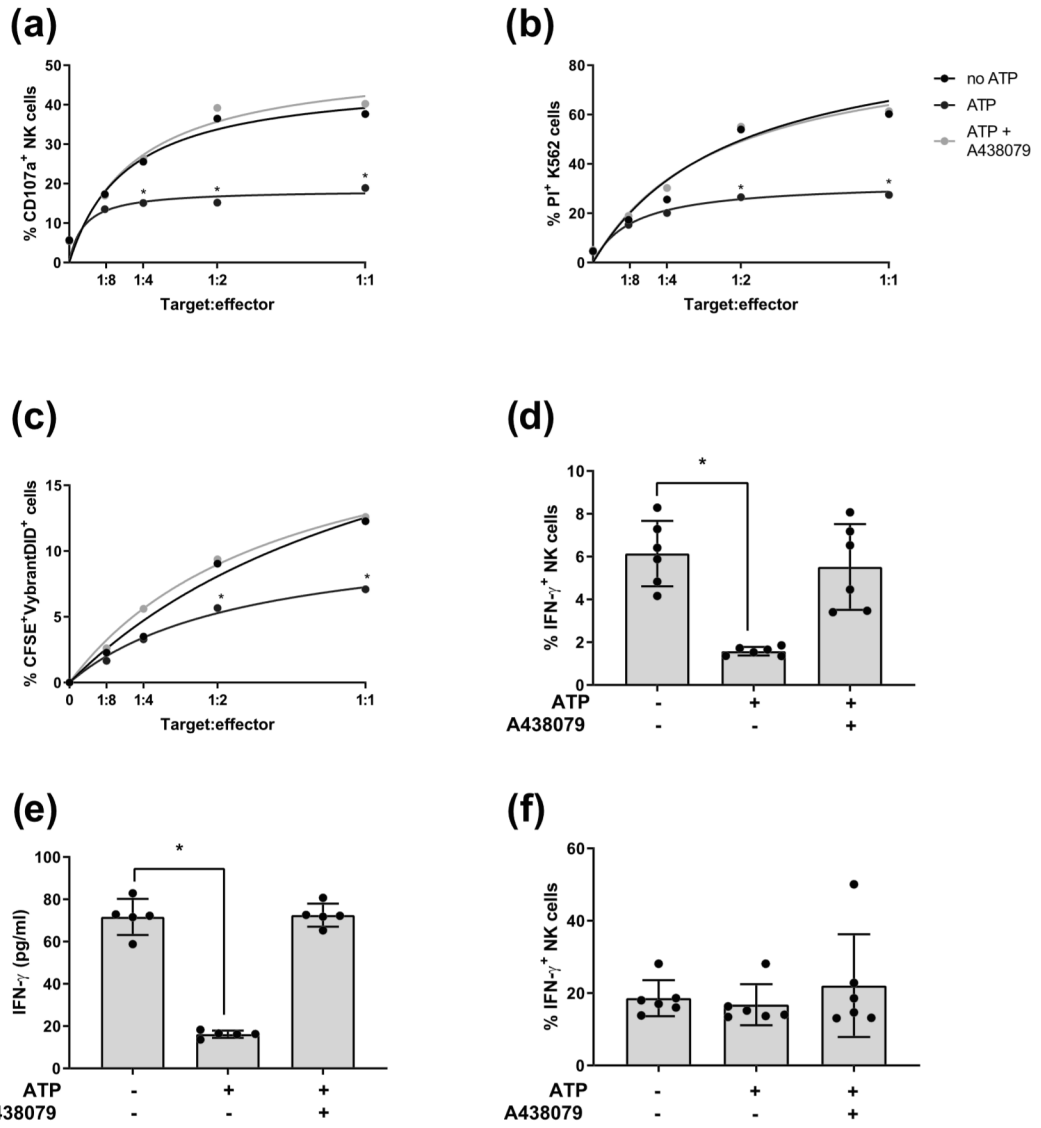

FIGURE 2 P2X7 activation induce a decrease in the antitumour activity of human natural killer (NK) cells. (a) NK cell degranulation as measured by the surface expression of CD107a. Isolated NK cells were incubated with or without 3-mM ATP, in the presence or absence of 50-μM A438079. Then, they were cocultured with carboxy-fluorescein diacetate succinimidyl ester (CFSE) stained K562 target cells at different target/effector (T/E) ratios. n = 5. (b) K562 cell killing determined as the percentage of $CFSE^{+}PI^{+}$ cells. NK cells and CFSE stained K562 were co-cultured as in *a*. n = 5. (c) NK/K562 conjugation measured as the percentage of $CFSE^{+}VybrantDID^{+}$ double positive events by flow cytometry. Vybrant™ DID stained NK cells were incubated with CFSE stained K562 at different E/T ratios for 20 min at room temperature. n = 5. (d) Intracellular IFN-γ expressing NK cells after 4-h incubation with CFSE stained K562 at 1:2 T/E ratio. n = 6. (e) IFN-γ secreted by NK cells that were incubated for 16 h in the presence of 200-U·ml^{-1} IL-2 and 20-ng·ml^{-1} IL-12, as measured by ELISA. n = 5. (f) Percentage of NK cells expressing intracellular IFN-γ. isolated NK cells (5×10^4 cells per well) were cultured for 6 h in the presence of 10-ng·ml^{-1} phorbol 12-myristate 13-acetate (PMA) and 500-ng·ml^{-1} ionomycin. n = 6. Results are presented as the mean ± SD; *$P \leq 0.05$; one-way ANOVA followed by Bonferroni test.

3.2 | P2X7 activation decrease the antitumour activity and IFN-γ secretion of NK cells

We next aimed to analyse the effect of P2X7 in the function of NK cells testing the cytotoxicity ability of NK cells over tumour cells. When NK cells (effector cells) were pretreated with ATP and co-cultured with the erythroblastoid target cell line K562, the frequency of degranulated cells was significantly lower compared with non-treated NK cells, at different E/T ratios (Figure 2a). Similarly, we found reduced killing of K562 cells when NK cells were pretreated with ATP (Figure 2b). In both cases, incubation with A438079 restored the anti-tumour activity of NK cells (Figure 2a,b). NK-tumour cell conjugation, the first step for the killing process (Orange, 2008), was also impaired after P2X7 stimulation, whereas A438079 reversed that impairment (Figure 2c). The production of IFN-γ by NK cells induced by tumour cells was decreased when NK cells were previously incubated with

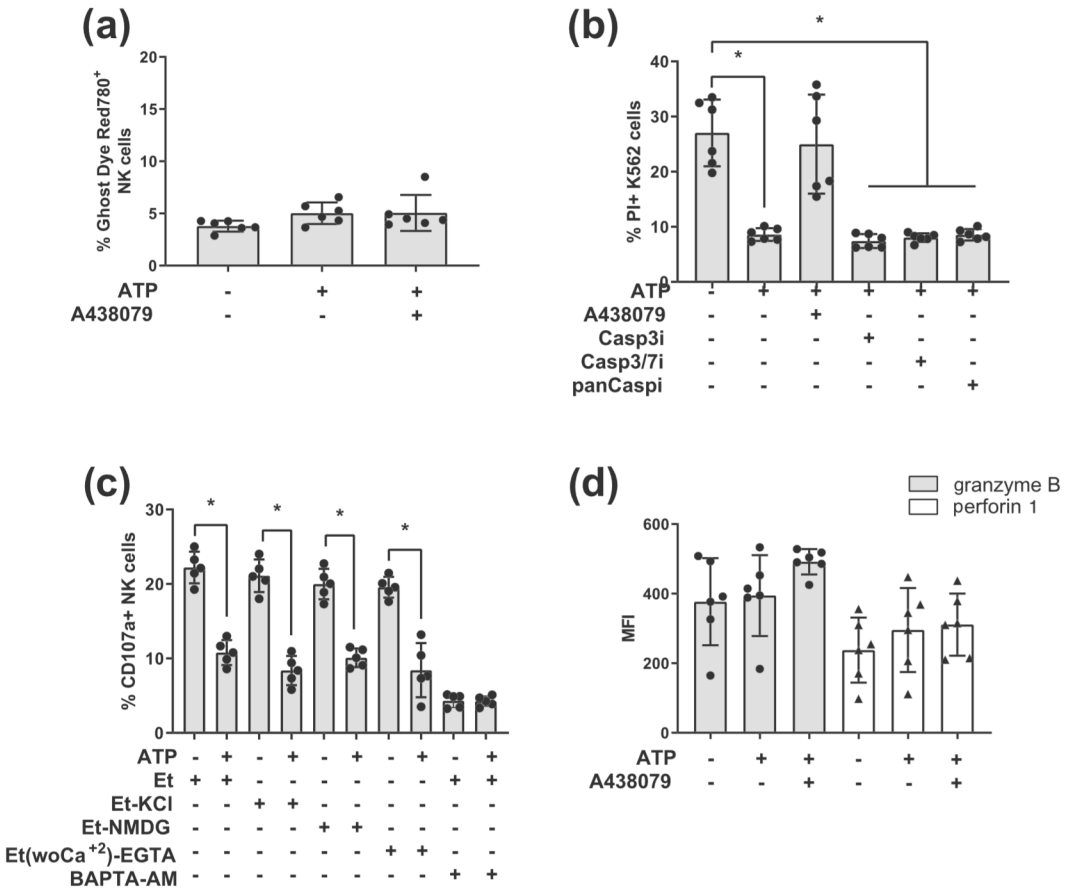

FIGURE 3 P2X7 activation does not induce human natural killer (NK) cell death. (a) Percentage of dead NK cells measured by flow cytometry. Isolated NK cells underwent 30-min incubation with 3-mM ATP. Then they were washed and stained with the viability dye ghost dye Red780. Dead cells were determined as highly positives for this viability dye. n = 6. (b) K562 cell death was determined as in *2b*. Isolated NK cells were previously treated with 3-mM ATP in the presence of different caspase inhibitors (caspase-3, caspase-3/7 (DICA) or a pan-caspase inhibitor (Z-VAD-FMK)). n = 6. (c) NK cell degranulation was determined as in *2a*. Isolated NK cells were incubated in different buffers: Et (Barbera-Cremades et al., 2012); Et-KCl (Et buffer with high concentration of potassium; 150-mM KCl); Et-NMDG (NaCl is replaced by N-methyl-D-glucamine), Et ($woCa^{+2}$)-EGTA ($CaCl_2$ depleted Et buffer with 1-mM ethylene glycol tetraacetic acid) or Et buffer with 100-μM cell permeant calcium chelator BAPTA-AM and activated with 3-mM ATP, washed, resuspended in culture medium and co-cultured with carboxy-fluorescein diacetate succinimidyl ester (CFSE) stained K582 cells (1:2 T/E ratio) in a standard 4-h cytotoxicity assay. n = 5. (d) Intracellular granzyme B and perforin 1 expression in isolated NK cells after ATP activation, measured as mean fluorescent intensity (MFI) by intracellular flow cytometry. n = 6. Results are presented as the mean ± SD; *$P \leq 0.05$; one-way ANOVA followed by Bonferroni test.

ATP and restored by A438079 (Figure 2d). P2X7 activation also impaired IFN-γ production induced by incubation with IL-2 and IL-12 cytokines (Figure 2e), but not by PMA/ionomycin, a strong and non-specific *activator of* NK cells (Figure 2f).

3.3 | P2X7 activation may regulate the surface expression and triggering effects of activating receptors CD16 and NKp46

To evaluate if the decreased antitumour activity of NK cells after ATP treatment is due to the cytotoxic effects of P2X7 (Volonte et al., 2012), we measured NK cell viability after 30 min of ATP stimulation, not finding differences in cell death when compared to untreated cells (Figure 3a). Moreover, NK cells incubated with different caspase inhibitors were not able to display their cytotoxic ability after ATP treatment (Figure 3b).

Signalling triggered by P2X7 results in a fast cellular cation exchange, including an efflux of K^+, and influx of Na^+ and Ca^{2+} into the cell (Surprenant & North, 2009). Consequently, we induced selective impairment of the different cation flux, using specific extracellular buffers. Our results showed that these treatments failed to restore the NK cells cytotoxicity activity, both analysed as NK cell degranulation (Figure 3c) or tumour cell killing (Figure S2a). Moreover, the presence of a cell permeant chelator with high Ca^{+2} selectivity, completely inhibited the cytotoxicity activity of NK cells, even in the absence of ATP (Figures 3c and S2a). Furthermore, P2X7 activation also induces the exocytosis of secretory lysosomes (Dubyak, 2012). To assess if NK cells could release granzyme B and perforin 1 granules after P2X7 activation, we measured their intracellular amount by

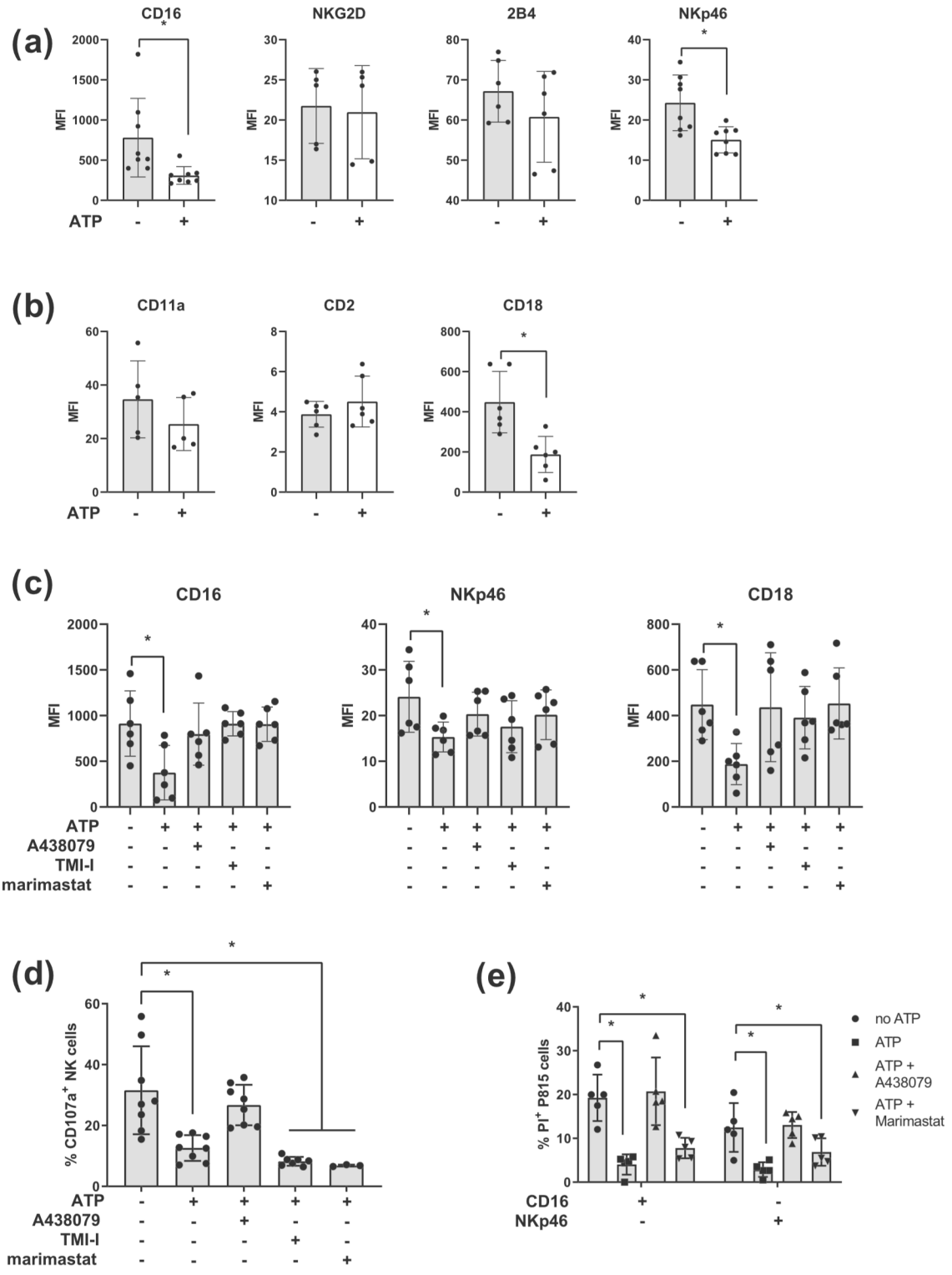

FIGURE 4 Legend on next page.

FIGURE 4 P2X7 activation induces the shedding of activating receptors CD16, NKp46 and integrin β2. (a, b) Expression of activator receptors CD16, NKG2D, 2B4 and NKp46 (a) or integrins CD2, CD11a (αL) and CD18 (β2) (b) in fresh and ATP treated natural killer (NK) cells measured as mean fluorescent intensity (MFI) by flow cytometry. n = 5–8. (c) Effect of metalloprotease inhibitors on CD16, NKp46 and integrin β2 surface expression in ATP-treated NK cells. Metalloprotease inhibitors were used at 30-μM TMI-I (ADAM17 inhibitor) or 50-μM marimastat (pan metalloprotease inhibitor). n = 6. (d) NK cell degranulation in the presence of metalloprotease inhibitors was determined as in *2a*. Isolated NK cells, treated with 3-mM ATP in the presence of 50-μM A438079, 30-μM TMI-I or 50-μM marimastat, were co-cultured with carboxyfluorescein diacetate succinimidyl ester (CFSE) stained K582 cells (1:2 T/E ratio) in a standard 4-h cytotoxicity assay. n = 8. (e) Reverse ADCC assay triggered by CD16 and NKp46 activating receptors. Isolated NK cells were pretreated with 3-mM ATP in the presence of 50-μM A438079 or 50-μM marimastat and then co-cultured with CFSE stained P815 cells (1:2 T/E ratio) for 4 h in the presence of anti-CD16, anti-NKp46 or IgG isotype control. P815 cell killing was determined as the percentage of $CFSE^{+}PI^{+}$ cells relative to basal cell death mediated by IgG isotype control in each condition. n = 5. Results are represented as the mean ± SD; $^{*}P \leq 0.05$; unpaired Student's *t* test (a, b) or one-way ANOVA followed by Bonferroni test (c–e).

intracellular flow cytometry. We found that ATP did not induce an intracellular decrease of these proteins (Figure 3d).

Additionally, P2X7 induces the activation of several metalloproteases, including matrix metalloproteinase (MMP) 9 (**MMP9**) (Gu & Wiley, 2006) and a disintegrin and metalloproteinase (ADAM) 17 (**ADAM17**) (Amores-Iniesta et al., 2017), whereas metalloproteases induce the shedding of membrane receptors in NK cells (Peruzzi et al., 2013; Wu et al., 2019; Zingoni et al., 2020). We found that ATP induced a partial but significant shedding of CD16 and NKp46 from NK cells but did not affect the surface expression of NKG2D or 2B4 (Figure 4a). CD16 and NKp46 ATP-induced shedding was reversed in the presence of A438079, or MMP inhibitors such as the specific ADAM17 inhibitor TMI-I, and the pan-MMP inhibitor marimastat (Figure 4c). P2X7 receptor also induced a MMP-dependent partial release of the β2 integrin CD18, a subunit of the LFA-1 integrin, a key component in the lytic immunologic synapse of NK cells (Orange et al., 2003) (Figure 4b,c). However, no shedding of either αL integrin CD11a, the other subunit of LFA-1, or CD2 was observed (Figure 4b). However, MMP inhibitors added during ATP treatment were not able to restore the conjugation between NK and K562 tumour cells (Figure S2b) and the NK cell antitumour activity as assayed by CD107a surface expression (Figure 4d) or K562 cell death (Figure S2c).

We also found that the signalling triggered by CD16 and NKp46 activating receptors was affected after ATP stimulation as assessed by reverse ADCC killing assay. Thus, P2X7 activation strongly inhibited the killing of P815 target cells triggered by CD16 (84.2%) and NKp46 (76.8%) NK cell activating receptors (Figure 4e), as compared with shedding results (60.4% and 36.8%, respectively, Figure 4a). This effect was completely reverted by the addition of A438079, but only partially reversed by the pan-MMP inhibitor marimastat (Figure 4e). Altogether, these results suggest that ATP-induced P2X7 activation may regulate the surface expression and the signalling pathway triggered by CD16 and NKp46 NK activating receptors and the expression of LFA-1, both mechanisms involved in NK-mediated tumour cell killing.

3.4 | P2X7 induces a long lasting irreversible anergic state of NK cells

To know the extent of ATP effects in human NK cells, we first tested their recovery for 2 h in culture after the 30-min treatment with ATP. As shown in Figure 5a, this time had no effect in the decrease of NK cells degranulation or even in K562 cell killing (Figure S3a). Again, no differences in NK cell death were found among treatments (Figure 5b). We next analysed the viability of these cells after P2X7 activation, so we followed the proliferation of NK cells for 5 days of culture in the presence of IL-2 or IL-15 after 30 min of ATP treatment. In all conditions, ATP pretreated NK cells had a lesser proliferation capacity compared to control or ATP plus A438079 treated cells (Figure 5c). Addition of IL-21 together with IL-2 or IL-15 had no effect on the proliferation of NK cells (Figure 5c). Strikingly, after those 5 days, percentages of living NK cells were similar in all treatment conditions, again indicating that ATP pretreatment does not affect viability of NK cells (Figure 5d). When we analysed the antitumour activity of these cells after the 5 days of proliferation, we could observe a slight recovery of the ability to kill K562 cells by previously ATP treated NK cells (day 0), but still lower than control and ATP plus A438079 treated cells (Figure 5e). After ATP treatment, NK cells were therefore non-proliferative but alive, somehow anchored in an anergic state. Anergic NK cells have previously been described in tumour environments, and anergy could be reversed by cytokine therapy (Ardolino et al., 2014). However, as shown in Figure 5f, incubation for 16 h with IL-12 and IL-18 after ATP treatment did not reverse the effect of ATP on the NK cell antitumour capacity. It should be pointed out that, in this case, the viability of NK cells was lower in ATP treated compared with control or ATP plus A438079 treated cells, in all conditions (Figure S3b).

3.5 | Genetic deletion of *P2rx7* increase antitumour activity of NK cells in vivo

Extracellular ATP concentration is elevated in the core of solid tumours (Pellegatti et al., 2008), and thus, we wondered if this could affect the antitumour activity of NK cells in a mouse model of solid tumour. P2X7 activation in mouse NK cells also results in a decrease of their antitumour activity against YAC-1 target cells (Figure S4a). Based on this premise, we designed an in vivo solid tumour mouse model with depleted $CD8^{+}$ T cells (Figure S4b) in C57/BL6 and C57/BL6-*P2rx7*$^{-/-}$ mice by subcutaneous injection of the melanoma cell line B16-F10 (Figure 6a). Ten days after injection,

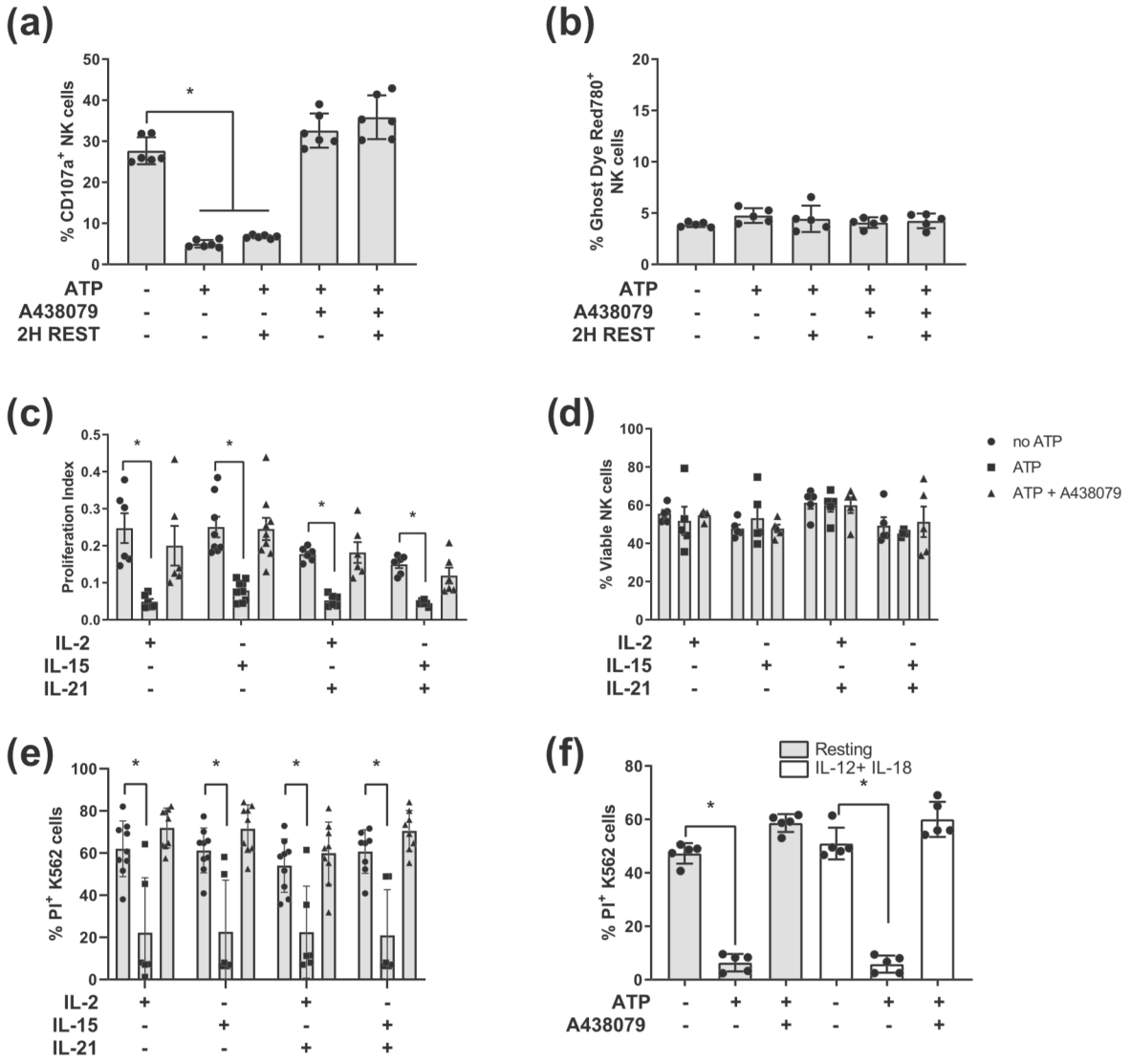

FIGURE 5 P2X7 activation induce a long lasting and not reversible anergic state in human resting natural killer (NK) cells. (a) NK cell degranulation was determined as in *2a*. Isolated NK cells were incubated with 3-mM ATP for 30 min and then washed and resuspended in culture medium. ATP treated NK cells were used directly, or after 2-h incubation in resting conditions (2H REST), and then co-cultured with carboxy-fluorescein diacetate succinimidyl ester (CFSE) stained K582 cells for 4 h at 1/2 T/E ratio. n = 6. (b) Percentage of dead NK cells measured by flow cytometry. Isolated ATP-treated NK cells were stained with the dye Ghost Dye Red780 for 30 min. Dead cells were determined as those highly positives for this viability dye. n = 5. (c–e) Isolated NK cells were pre-incubated with 3-mM ATP in the presence (grey bars) or absence (white bars) of 50-μM A438079 for 30 min, washed, resuspended in culture medium and then 10^4 (c), 5×10^4 (d) or 10^5 (e) NK cells were cultured for 5 days with 200-U·ml^{-1} IL-2 or 25-ng·ml^{-1} IL-15, with or without 50-ng·ml^{-1} IL-21. Proliferation (c; n = 6), Ghost Dye780$^{dim/-}$ viable NK cells (d; n = 5) or the cytotoxicity capacity (e; n = 6) of these NK cells was measured after those 5 days of culture. For the NK cytotoxicity assay, 5×10^4 alive proliferating NK cells were co-cultured with 2.5×10^4 CFSE stained K562 cells (1:2 T/E ratio) for 4 h. (f) K562 cell death was determined as in *2b*. Isolated human NK cells were incubated with 3-mM ATP for 30 min and then washed and resuspended in culture medium. The 5×10^4 activated NK cells were maintained rested or activated with 20-ng·ml^{-1} IL-12 and 50-ng·ml^{-1} IL-18 for 16 h. After that, NK cells were co-cultured with 2.5×10^4 CFSE stained K562 cells (1:2 T/E ratio) for 4 h. n = 5. Results are presented as the mean ± SD; *$P \leq 0.05$; one-way ANOVA followed by Bonferroni test.

tumour volume and weight from *P2xr7*$^{-/-}$ mice were smaller than those observed in C57/BL6 wild-type mice (Figure 6b). Tumour size was recovered when NK cells were depleted from the *P2rx7*$^{-/-}$ mice by anti-NK1.1 clone PK136 antibody treatment, but not for wild-type mice (Figures 6b and S4c). Furthermore, increased infiltrating NK cells were found in the tumour developed in the *P2rx7*$^{-/-}$ mice when analysed by immunohistochemistry (Figure 6c). However, the *P2rx7*$^{-/-}$ mice presented a similar percentage of NK cells than C57/BL6 wild-type mice in the spleen (Figure S4d).

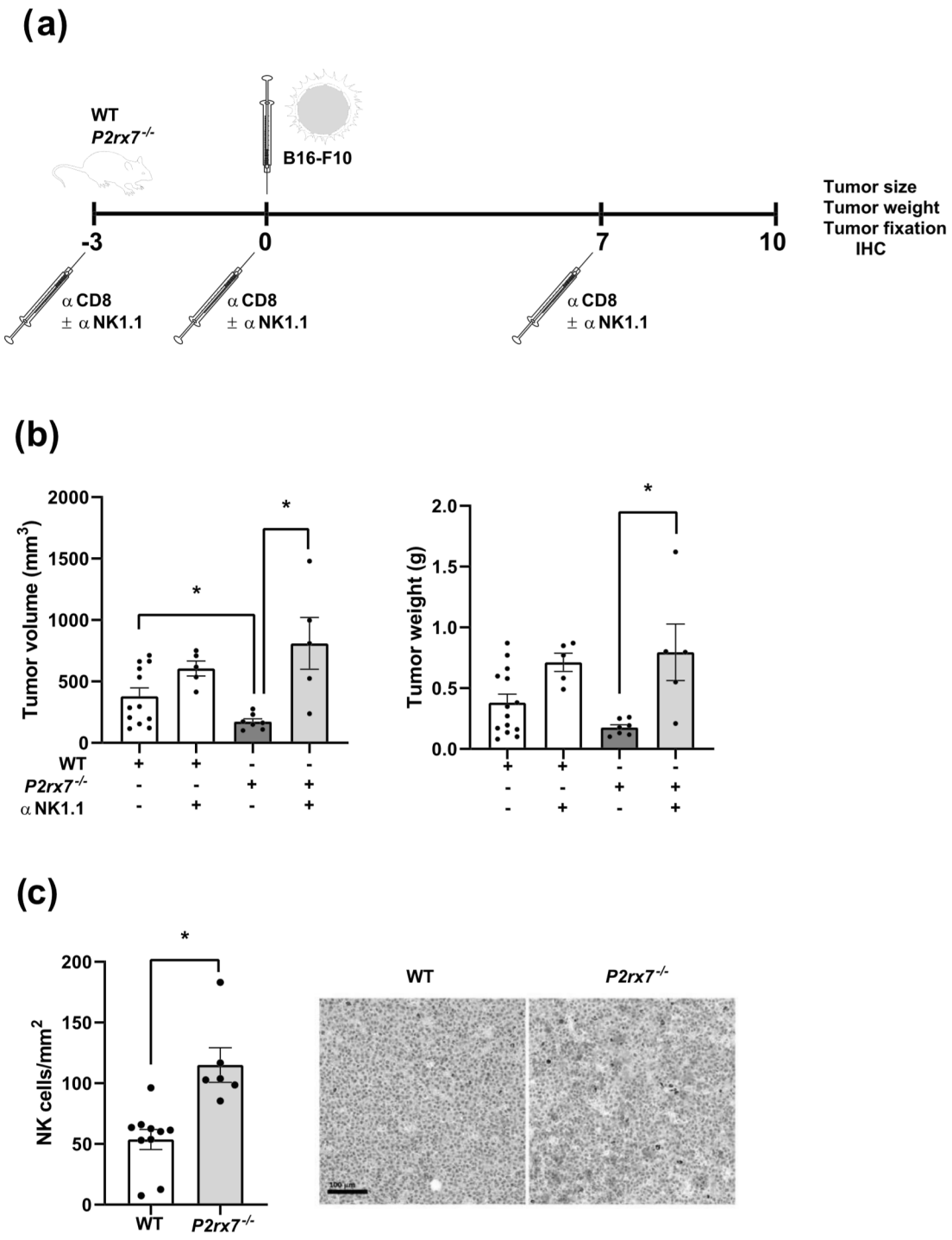

FIGURE 6 Genetic deficiency of *P2rx7* induce a higher antitumour capacity of natural killer (NK) cells in a model of solid tumour in mice. (a) Schematic representation of the solid tumour mouse model performed by the injection of 10^6 B16-F10 cells. CD8 + cells were depleted by i.p. injection of 100-μg anti-CD8β clone 53–5.8 at days −3, 0 and +7. Where indicated, NK cells were also depleted by co-injection of 100-μg anti-NK1.1 clone PK136 at the same 3 days. (b) Volume and weight of solid tumours extracted from mice after 10 days of inoculation. The minimum number of mice necessary to obtain statistically significant differences among groups was used (n = 12 per WT group; n = 7 per *P2rx7*$^{-/-}$ group and n = 5 per *P2rx7*$^{-/-}$ treated with αNK1.1). (c) Infiltrated NK cell number per mm^2 of the solid tumour. Three 20× random fields were analysed from each tumour. Two representative 20× pictures of tumours coming from WT or *P2xr7*$^{-/-}$ mice are shown. n = 10 per WT group and n = 8 per *P2rx7*$^{-/-}$ *group*. Each dot represents a single mouse (b) or tumour (c). Results are presented as the mean ± SD; *$P \leq 0.05$; unpaired Student's *t* test (c) or one-way ANOVA followed by Bonferroni test (b).

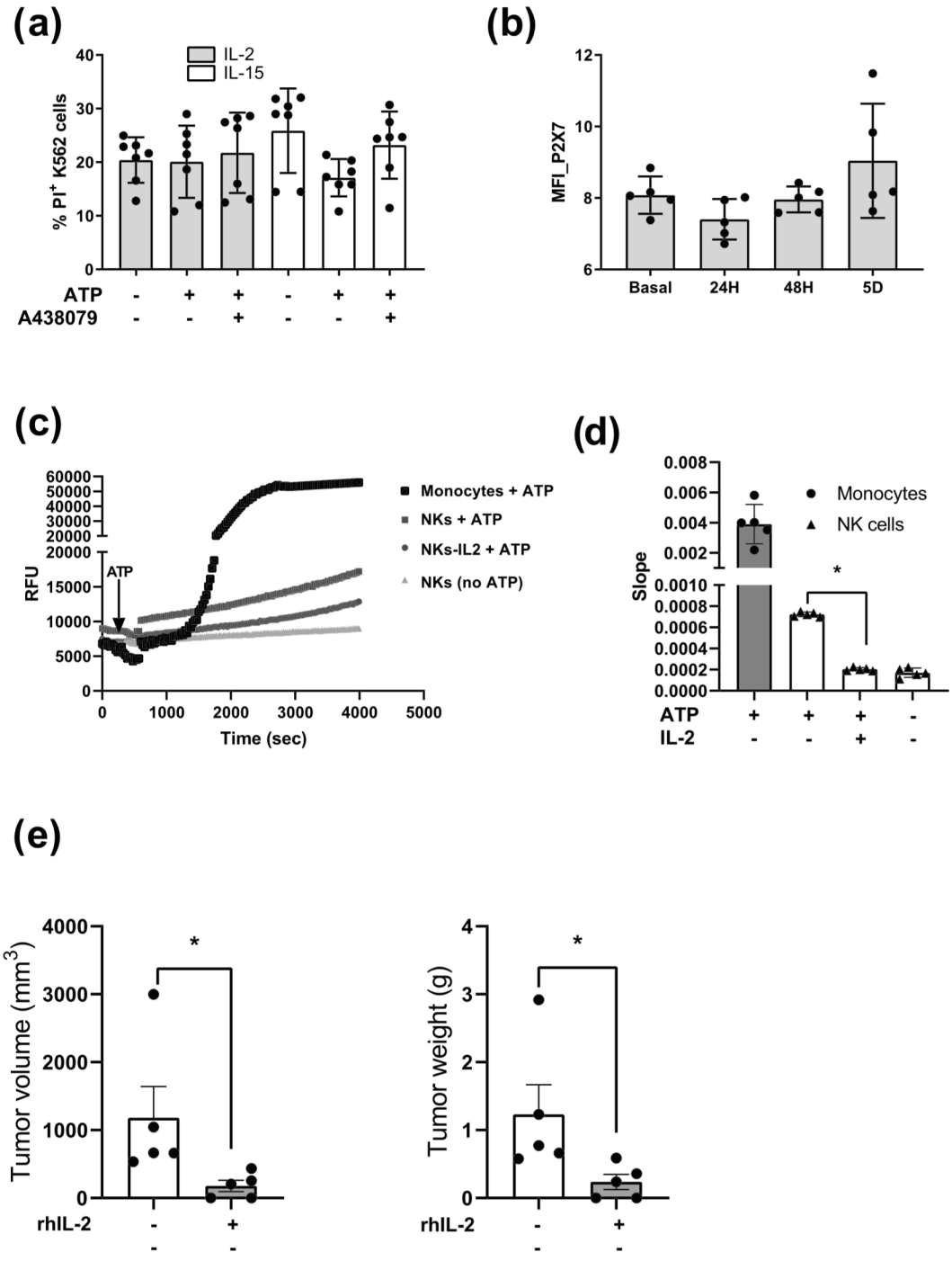

FIGURE 7 IL-2 and IL-15 activated natural killer (NK) cells maintain antitumour capacity after ATP treatment. (a) K562 cell death determined as in *2b*. Isolated human NK cells were cultured for 5 days in the presence of 200-U·ml^{-1} IL-2 or 25-ng·ml^{-1} IL-15. After those 5 days of culture, NK cells were treated with 3-mM ATP for 30 min in the presence or absence of 50-μM A438079. Then, 5 × 10^4 living NK cells were co-cultured with 2.5 × 10^4 carboxy-fluorescein diacetate succinimidyl ester (CFSE) stained K562 cells (1:2 T/E ratio) for 4 h. n = 7. (b) P2X7 expression in NK cells as detected by flow cytometry. Isolated human NK cells, cultured for several days in the presence of 200-U·ml^{-1} IL-2, were stained for P2X7 membrane expression using the L4 clone antibody. n = 5. (c, d) Kinetics of Yo-Pro uptake expressed as relative fluorescent units (RFU) (c; representative kinetic graph is shown from five independent experiments.) and the intracellular Ca^{+2} increase expressed as the slope of the exponential Fura-2-AM signal recorded over time (d; n = 5) in isolated NK cells and monocytes. NK cells were assayed in resting conditions (NKs) or after 5 days of proliferation in the presence of 200-U·ml^{-1} IL-2 (NKs-IL2). (e) WT CD8-depleted tumour-inoculated mice were treated daily with 5000 U of recombinant human IL-2 (rhIL-2) from day 0 until day 4 and compared with non-treated mice. Volume and weight for the solid tumour extracted from mice after 10 days of inoculation was calculated such as in Fig.*6c*. The minimum number of mice necessary to obtain statistically significant differences among groups was used (n = 5 per group). Each dot represents a single mouse. Results are presented as the mean ± SD; *$P \leq 0.05$; unpaired Student's *t* test (e) or one-way ANOVA followed by Bonferroni test (a, b and d).

3.6 | NK cell activation with cytokines impairs the inhibitory effect of P2X7

Immunotherapies based on NK cells are among the most promising therapies under development for the treatment of incurable forms of leukaemia and other types of cancer (Hofer & Koehl, 2017). Ex vivo culture of NK cells with cytokines such as IL-2 and IL-15 is a clinical approach that allows significant expansion of NK cell subpopulations, which are likely to have potent antitumour effects (de Rham et al., 2007). Therefore, we wondered whether activation in the presence of IL-2 or IL-15 affected extracellular ATP-induced P2X7 function in human NK cells. After 5 days of culture in the presence of IL-2 or IL-15, P2X7 activation did not affect the ability of NK cells to kill tumour K562 cells (Figure 7a). During this time, no changes in NK cell P2X7 expression were appreciated (Figure 7b). However, IL-2 activation reduced YO-PRO-1 uptake and intracellular Ca^{2+} rise after P2X7 activation (Figure 7c,d). Moreover, $CD8^+$ T cells depleted wild type mice, treated with high-dose of recombinant IL-2 (Zloza et al., 2017) for the first 5 days after tumour inoculation, presented a reduction in the tumour size, compared with untreated group (Figure 7e) and similar to what was found in *P2rx7*$^{-/-}$ mice (Figure 6b). Altogether, our study demonstrates that P2X7 activation reduces antitumour function in NK cells and supports the beneficial effects of IL-2 or IL-15 therapies.

4 | DISCUSSION

NK cells represent a first line of defence against tumours, and there is a positive correlation between high intratumoural levels of NK cells and increased survival to several types of cancer (Senovilla et al., 2012). Therefore, NK cells-based immunotherapy strategies are among the most promising treatments against several types of cancer (Hofer & Koehl, 2017). However, tumour-infiltrating NK cells associated with advanced disease may have profound functional defects, indicating that NK cell function is critically altered during cancer progression (Stabile et al., 2017). Death and stressed cells often release ATP and other nucleotides into the extracellular space, reaching high extracellular concentrations in inflamed areas and in the core of solid tumours (Pellegatti et al., 2008). Furthermore, it has been confirmed that this released ATP triggers P2X7 signalling in different tumour-associated immune cells (De Marchi et al., 2019). P2X7 signalling in lymphocytes can induce activation or inhibition depending on the ATP concentration and the activation state of P2X7 (Burnstock & Boeynaems, 2014). Our results show that extracellular ATP impairs NK cytotoxic activity, in agreement with early studies (Henriksson, 1983; Schmidt et al., 1984). This effect is mainly mediated by P2X7 activation that occurs at millimolar concentrations of ATP, unlike other studies where lower concentrations were used and were mediated by **P2Y11** receptor activation (Gorini et al., 2010; Henriksson, 1983; Schmidt et al., 1984). Although we cannot exclude the involvement of other P2 receptors in our results, our data point to P2X7 as the receptor on NK cells that inhibits its antitumour activity. A438079, a specific and competitive P2X7 antagonist (Donnelly-Roberts & Jarvis, 2007), was able to restore immune function of ATP-treated NK cells. P2X7 activation induces diverse cellular signalling cascades, ranging from intracellular Ca^{2+} rise, cell death, cell blebbing, microparticle shedding, MMP activation, intravesical exocytosis or the shedding of plasma membrane ligands (Mishra et al., 2021). However, none of the downstream effects of P2X7 activation appeared to be involved in the inhibition of NK cell function. Nevertheless, P2X7 triggering induced MMP-dependent partial shedding of the CD16 and NKp46 activating receptors as well as the adhesion molecule CD18. Strikingly, CD16 and NKp46 killing action against P815 targets was strongly reduced in ATP treated NK cells that could not be simply explained by the partial shedding of both activating receptors. Therefore, our results suggest a P2X7 role modulating NK cytotoxicity triggered by CD16 and NKp46. Both receptors share the same activation signalling cascade due to their common coupled adapter molecules FcεRIγ (Watzl & Long, 2010). Concurrently, target cells K562 are known for expressing abundant ligands for NKp46, **NKp30** (another FcεRIγ coupled activating receptor) as well as **ICAM-1** and **ICAM-2** counter-receptors of the LFA-1 adhesion molecule (Tremblay-McLean et al., 2019). Therefore, we conclude that P2X7 may regulate the signalling pathway triggered by NK activating receptors such as CD16 and NKp46.

Likewise, our results show that extracellular ATP impairs IFN-γ production. IFN-γ promotes T helper 1 cells differentiation and cytotoxic T lymphocytes functions against tumour cells, whereas it can reduce tumour cell proliferation and sensitize pro-apoptotic pathways regulating the expression of Fas/FasL, TNF-related apoptosis-inducing ligand (TRAIL), and caspases, among others. Furthermore, IFN-γ can disturb the proliferation and survival of endothelial cells and hamper angiogenesis in the tumour micro-environment (Kursunel & Esendagli, 2016).

Ca^{2+} influx through store-generated channels is indispensable for lytic granule release (Krzewski & Coligan, 2012). **Phospholipase Cγ1**-generated **inositol-(1,4,5)-triphosphate** (IP_3) after formation of immune synapse, induces the release of Ca^{2+} from the intracellular store and aggregation of the endoplasmic reticulum Ca^{2+} sensor STIM1. This leads to activation of the Ca^{2+} channel **Orai1** and Ca^{2+} influx from an extracellular medium (Schwarz et al., 2013). However, an optimal Ca^{2+} balance is required for NK cell cytotoxicity (Zhou et al., 2018). Thus, intracellular Ca^{2+} rise caused by P2X7 activation, previous to immune synapse formation, might result in unbalanced intracellular Ca^{2+} concentration, leading to poor antitumour activity of NK cells. However, our results in the absence of extracellular Ca^{2+} do not support this claim. Nevertheless, HEK293 cells transfected with P2X7 release a larger amount of Ca^{2+} from intracellular stores after stimulation of plasma membrane receptors coupled to IP_3 generation (Adinolfi, Callegari, et al., 2005).

P2X7 activation affected NK/K562 conjugates formation and NK cytotoxic function likely regulating the signalling pathway triggered by NK activating receptors. Therefore, P2X7 activation evokes an apparently anergic state that could be found in intratumoural NK cells (Ardolino et al., 2014). Tumour-induced NK anergy is reversed by

cytokines, a successful and promising treatment for certain types of cancer (Ardolino et al., 2014). Several cellular approaches use NK cells in long-term ex vivo cultures with recombinant cytokines, including IL-2 and IL-15, to treat cancer (Hofer & Koehl, 2017). Non-functional isoforms of P2X7 have been described in cancer cells (Gilbert et al., 2019). Our results indicate that IL-2 treated NK cells, despite expressing equal P2X7 at plasma membrane, display a non-functional P2X7 unable to open the non-specific cation-selective pore and thus increase intracellular Ca^{2+}. However, that could not be differentiated from functional P2X7 with the antibody used in our study (Barden et al., 2003; Surprenant et al., 1996). Many clinical trials to treat solid tumours are based on the adoptive transfer of autologous ex vivo expanded NK cells co-infused with recombinant IL-2 (van Vliet et al., 2021). Although relevant results have been obtained in patients with advanced melanoma and other solid tumours, the severe IL-2-related toxicity and the IL-2-induced expansion of Tregs limit the generalized use of this type of therapies. This limitation may be overcome by the use of recombinant IL-15 instead of IL-2 (Sivori et al., 2021). Therapeutic IL-15 administration does not cause vascular leak syndrome nor activate Tregs, although some other side effects have been found in early phase clinical trials (Lee et al., 2021). Nevertheless, mutant forms of recombinant IL-2 with a high affinity for the IL-2Rβγ receptor present on NK cells, but reduced affinity for the IL-2Rα receptor expressed on Tregs, are also emerging as alternative therapies to induce NK activation without inducing Treg-mediated immunosuppression (Sim et al., 2016). Our data suggest that in all these therapies, the presence of a non-functional P2X7 will help in the antitumour activity of infused NK cells. Beyond infusion of expanded NK cells, recent development of chimeric antigen receptor (CAR)-engineered NK cells (CAR-NK) is a promising cellular immunotherapy for cancer (Xie et al., 2020). Our results open the possibility that P2X7 manipulation for the expression of a non-functional P2X7 may result in the generation of better CAR-NK cells resistant to ATP-induced anergy and superior antitumour capacity. Likewise, and although controversy does exist about the role of P2X7 splice-variants or single-nucleotide polymorphisms (SNPs) in oncogenesis (Pegoraro et al., 2021), the analysis of these variants or mutations inducing nonfunctional or loss-of-function P2X7 in NK cells, may help to stratify cancer patients with a better prognosis.

In contrast to previous studies in which *P2xr7*$^{-/-}$ mice showed an accelerated tumour progression (Adinolfi et al., 2015; Yan et al., 2020) and a decrease in tumour infiltration of $CD8^+$ T cells (De Marchi et al., 2019), our solid tumour model exhibited a reduction in tumour size associated with NK cells. It is worth noting that we developed a solid tumour model with depletion of $CD8^+$ cells, to boost NK cells action. In this regard, in a mouse starting with lower numbers of tumour infiltrating $CD8^+$ cells, the effect of their depletion on tumour dimension could be less critical than seen in wild-type mice. Nevertheless, the depletion of NK cells in addition to $CD8^+$ cells did not have a great effect in the tumour growth in wild-type mice, so indicating the limited capacity of P2X7 wild-type NK cells to control solid tumour growth. Likewise, although using B16-F10 cells as a model, we injected more cells into mice and sacrificed them at earlier time points compared to those previous studies, such as the infiltration of immune cells might vary at different times of tumour development (Cali et al., 2017). Furthermore, some key differences have already been shown comparing different *P2xr7*$^{-/-}$ strains (Masin et al., 2012; Taylor et al., 2009). Thus, whereas our model was developed in complete P2X7 null mice (Kaczmarek-Hajek et al., 2018), the aforementioned models were carried out in the *GlaxoSmithKline* knockout strain (Adinolfi et al., 2015; De Marchi et al., 2019) or *Pfizer* knockout strain (Yan et al., 2020).

Altogether, the results obtained in the present study show a new function of P2X7 in NK cells, decreasing their cytotoxic and immunomodulatory activity. That new function may be physiologically triggered by the high concentrations of ATP present in the tumour core, diminishing their antitumourigenic capacity and adding ATP signalling to the plethora of mechanisms involved in NK cell dysfunction in the tumour environment (Cozar et al., 2021). This phenomenon could be bypassed by the current therapies using recombinant IL-2 or IL-15 to expand therapeutic NK cells, paving the way for the future generation of novel CAR-NK cells with non-functional P2X7.

CONFLICT OF INTEREST

PP is co-inventor on patent application to use NLRP3 inflammasome as biomarker of disease, which have been licensed to Viva in vitro diagnostics SL, a company co-funded by PP and AB-M. PP is scientific consultant of Glenmark Ltd. The other authors declare no conflict of interests.

AUTHOR CONTRIBUTION

A. B-M. and P. P. participated in the design of the work. A. B-M., P. P. and T. H-C. participated in the discussion and review of the manuscript. A. B-M., F. L-R., A. P-F., C. dT-M., C. A-V. and T. H-C. carried out all the experiments and statistical analysis.

DECLARATION OF TRANSPARENCY AND SCIENTIFIC RIGOUR

This Declaration acknowledges that this paper adheres to the principles for transparent reporting and scientific rigour of preclinical research as stated in the *BJP* guidelines for Design and Analysis, Immunoblotting and Immunochemistry, and Animal Experimentation, and as recommended by funding agencies, publishers and other organizations engaged with supporting research.

DATA AVAILABILITY STATEMENT

The data that support the findings of this study are available from the corresponding author upon reasonable request. Some data may not be made available because of privacy or ethical restrictions.

ORCID

Alberto Baroja-Mazo https://orcid.org/0000-0001-5212-5006

REFERENCES

Adinolfi, E., Callegari, M. G., Ferrari, D., Bolognesi, C., Minelli, M., Wieckowski, M. R., Pinton, P., Rizzuto, R., & di Virgilio, F. (2005). Basal

activation of the P2X7 ATP receptor elevates mitochondrial calcium and potential, increases cellular ATP levels, and promotes serum-independent growth. *Molecular Biology of the Cell*, *16*(7), 3260–3272. https://doi.org/10.1091/mbc.e04-11-1025

Adinolfi, E., Capece, M., Franceschini, A., Falzoni, S., Giuliani, A. L., Rotondo, A., Sarti, A. C., Bonora, M., Syberg, S., Corigliano, D., Pinton, P., Jorgensen, N. R., Abelli, L., Emionite, L., Raffaghello, L., Pistoia, V., & di Virgilio, F. (2015). Accelerated tumor progression in mice lacking the ATP receptor P2X7. *Cancer Research*, *75*(4), 635–644. https://doi.org/10.1158/0008-5472.CAN-14-1259

Adinolfi, E., Pizzirani, C., Idzko, M., Panther, E., Norgauer, J., Di Virgilio, F., & Ferrari, D. (2005). P2X(7) receptor: Death or life? *Purinergic Signal*, *1*(3), 219–227. https://doi.org/10.1007/s11302-005-6322-x

Alexander, S. P., Kelly, E., Mathie, A., Peters, J. A., Veale, E. L., Armstrong, J. F., Faccenda, E., Harding, S. D., Pawson, A. J., Southan, C., & Buneman, O. P. (2021). THE CONCISE GUIDE TO PHARMACOLOGY 2021/22: Introduction and other protein targets. *British Journal of Pharmacology*, *178*(Suppl 1), S1–S26. https://doi.org/10.1111/bph.15540

Alexander, S. P., Mathie, A., Peters, J. A., Veale, E. L., Striessnig, J., Kelly, E., Armstrong, J. F., Faccenda, E., Harding, S. D., Pawson, A. J., & Southan, C. (2021). THE CONCISE GUIDE TO PHARMACOLOGY 2021/22: Ion channels. *British Journal of Pharmacology*, *178*(Suppl 1), S157–S245.

Alexander, S. P. H., Roberts, R. E., Broughton, B. R. S., Sobey, C. G., George, C. H., Stanford, S. C., Cirino, G., Docherty, J. R., Giembycz, M. A., Hoyer, D., Insel, P. A., Izzo, A. A., Ji, Y., MacEwan, D. J., Mangum, J., Wonnacott, S., & Ahluwalia, A. (2018). Goals and practicalities of immunoblotting and immunohistochemistry: A guide for submission to the British Journal of Pharmacology. *British Journal of Pharmacology*, *175*(3), 407–411. https://doi.org/10.1111/bph.14112

Amores-Iniesta, J., Barbera-Cremades, M., Martinez, C. M., Pons, J. A., Revilla-Nuin, B., Martinez-Alarcon, L., Di Virgilio, F., Parrilla, P., Baroja-Mazo, A., & Pelegrín, P. (2017). Extracellular ATP activates the NLRP3 Inflammasome and is an early danger signal of skin allograft rejection. *Cell Reports*, *21*(12), 3414–3426. https://doi.org/10.1016/j.celrep.2017.11.079

Ardolino, M., Azimi, C. S., Iannello, A., Trevino, T. N., Horan, L., Zhang, L., Deng, W., Ring, A. M., Fischer, S., Garcia, K. C., & Raulet, D. H. (2014). Cytokine therapy reverses NK cell anergy in MHC-deficient tumors. *The Journal of Clinical Investigation*, *124*(11), 4781–4794. https://doi.org/10.1172/JCI74337

Aswad, F., & Dennert, G. (2006). P2X7 receptor expression levels determine lethal effects of a purine based danger signal in T lymphocytes. *Cellular Immunology*, *243*(1), 58–65. https://doi.org/10.1016/j.cellimm.2006.12.003

Barbera-Cremades, M., Baroja-Mazo, A., Gomez, A. I., Machado, F., Di Virgilio, F., & Pelegrin, P. (2012). P2X7 receptor-stimulation causes fever via PGE2 and IL-1beta release. *The FASEB Journal*, *26*(7), 2951–2962. https://doi.org/10.1096/fj.12-205765

Barden, J. A., Sluyter, R., Gu, B. J., & Wiley, J. S. (2003). Specific detection of non-functional human P2X(7) receptors in HEK293 cells and B-lymphocytes. *FEBS Letters*, *538*(1–3), 159–162. https://doi.org/10.1016/S0014-5793(03)00172-8

Bryceson, Y. T., & Ljunggren, H. G. (2011). Natural killer cells: Biology, physiology and medicine – Part 1. *Journal of Innate Immunity*, *3*(3), 213–215. https://doi.org/10.1159/000325332

Burnstock, G., & Boeynaems, J. M. (2014). Purinergic signalling and immune cells. *Purinergic Signal*, *10*(4), 529–564. https://doi.org/10.1007/s11302-014-9427-2

Cali, B., Molon, B., & Viola, A. (2017). Tuning cancer fate: The unremitting role of host immunity. *Open Biology*, *7*(4). https://doi.org/10.1098/rsob.170006

Cozar, B., Greppi, M., Carpentier, S., Narni-Mancinelli, E., Chiossone, L., & Vivier, E. (2021). Tumor-infiltrating natural killer cells. *Cancer Discovery*, *11*(1), 34–44. https://doi.org/10.1158/2159-8290.CD-20-0655

Curtis, M. J., Alexander, S., Cirino, G., Docherty, J. R., George, C. H., Giembycz, M. A., Hoyer, D., Insel, P. A., Izzo, A. A., Ji, Y., MacEwan, D. J., Sobey, C. G., Stanford, S. C., Teixeira, M. M., Wonnacott, S., & Ahluwalia, A. (2018). Experimental design and analysis and their reporting II: Updated and simplified guidance for authors and peer reviewers. *British Journal of Pharmacology*, *175*(7), 987–993. https://doi.org/10.1111/bph.14153

De Marchi, E., Orioli, E., Pegoraro, A., Sangaletti, S., Portararo, P., Curti, A., Colombo, M. P., Di Virgilio, F., & Adinolfi, E. (2019). The P2X7 receptor modulates immune cells infiltration, ectonucleotidases expression and extracellular ATP levels in the tumor microenvironment. *Oncogene*, *38*(19), 3636–3650. https://doi.org/10.1038/s41388-019-0684-y

de Rham, C., Ferrari-Lacraz, S., Jendly, S., Schneiter, G., Dayer, J. M., & Villard, J. (2007). The proinflammatory cytokines IL-2, IL-15 and IL-21 modulate the repertoire of mature human natural killer cell receptors. *Arthritis Research & Therapy*, *9*(6), R125. https://doi.org/10.1186/ar2336

de Torre-Minguela, C., Barbera-Cremades, M., Gomez, A. I., Martin-Sanchez, F., & Pelegrin, P. (2016). Macrophage activation and polarization modify P2X7 receptor secretome influencing the inflammatory process. *Scientific Reports*, *6*, 22586. https://doi.org/10.1038/srep22586

Donnelly-Roberts, D. L., & Jarvis, M. F. (2007). Discovery of P2X7 receptor-selective antagonists offers new insights into P2X7 receptor function and indicates a role in chronic pain states. *British Journal of Pharmacology*, *151*(5), 571–579. https://doi.org/10.1038/sj.bjp.0707265

Dou, L., Chen, Y. F., Cowan, P. J., & Chen, X. P. (2018). Extracellular ATP signaling and clinical relevance. *Clinical Immunology*, *188*, 67–73. https://doi.org/10.1016/j.clim.2017.12.006

Dubyak, G. R. (2012). P2X7 receptor regulation of non-classical secretion from immune effector cells. *Cellular Microbiology*, *14*(11), 1697–1706. https://doi.org/10.1111/cmi.12001

Ge, Z., Wu, S., Zhang, Z., & Ding, S. (2020). Mechanism of tumor cells escaping from immune surveillance of NK cells. *Immunopharmacology and Immunotoxicology*, *42*(3), 187–198. https://doi.org/10.1080/08923973.2020.1742733

Gilbert, S. M., Oliphant, C. J., Hassan, S., Peille, A. L., Bronsert, P., Falzoni, S., di Virgilio, F., McNulty, S., & Lara, R. (2019). ATP in the tumour microenvironment drives expression of nfP2X7, a key mediator of cancer cell survival. *Oncogene*, *38*(2), 194–208. https://doi.org/10.1038/s41388-018-0426-6

Gonzalez-Rodriguez, A. P., Villa-Alvarez, M., Sordo-Bahamonde, C., Lorenzo-Herrero, S., & Gonzalez, S. (2019). NK cells in the treatment of hematological malignancies. *Journal of Clinical Medicine*, *8*(10). https://doi.org/10.3390/jcm8101557

Gorini, S., Callegari, G., Romagnoli, G., Mammi, C., Mavilio, D., Rosano, G., Fini, M., di Virgilio, F., Gulinelli, S., Falzoni, S., Cavani, A., Ferrari, D., & la Sala, A. (2010). ATP secreted by endothelial cells blocks CX(3)CL 1-elicited natural killer cell chemotaxis and cytotoxicity via P2Y(1) (1) receptor activation. *Blood*, *116*(22), 4492–4500. https://doi.org/10.1182/blood-2009-12-260828

Gu, B. J., & Wiley, J. S. (2006). Rapid ATP-induced release of matrix metalloproteinase 9 is mediated by the P2X7 receptor. *Blood*, *107*(12), 4946–4953. https://doi.org/10.1182/blood-2005-07-2994

Gu, B. J., Zhang, W. Y., Bendall, L. J., Chessell, I. P., Buell, G. N., & Wiley, J. S. (2000). Expression of P2X(7) purinoceptors on human lymphocytes and monocytes: Evidence for nonfunctional P2X(7) receptors. *American Journal of Physiology. Cell Physiology*, *279*(4), C1189–C1197. https://doi.org/10.1152/ajpcell.2000.279.4.C1189

Henriksson, T. (1983). Inhibition of natural killing by adenosine ribonucleotides. *Immunology Letters*, *7*(3), 171–176. https://doi.org/10.1016/0165-2478(83)90066-4

Hofer, E., & Koehl, U. (2017). Natural killer cell-based cancer immunotherapies: From immune evasion to promising targeted cellular therapies. *Frontiers in Immunology*, *8*, 745. https://doi.org/10.3389/fimmu.2017.00745

Ingram, Z., Madan, S., Merchant, J., Carter, Z., Gordon, Z., Carey, G., & Webb, T. J. (2021). Targeting natural killer T cells in solid malignancies. *Cell*, *10*(6). https://doi.org/10.3390/cells10061329

Jacob, F., Perez Novo, C., Bachert, C., & Van Crombruggen, K. (2013). Purinergic signaling in inflammatory cells: P2 receptor expression, functional effects, and modulation of inflammatory responses. *Purinergic Signal*, *9*(3), 285–306. https://doi.org/10.1007/s11302-013-9357-4

Jamieson, G. P., Snook, M. B., Thurlow, P. J., & Wiley, J. S. (1996). Extracellular ATP causes of loss of L-selectin from human lymphocytes via occupancy of P2Z purinocepters. *Journal of Cellular Physiology*, *166*(3), 637–642. https://doi.org/10.1002/(SICI)1097-4652(199603)166:3<637::AID-JCP19>3.0.CO;2-3

Junger, W. G. (2011). Immune cell regulation by autocrine purinergic signalling. *Nature Reviews. Immunology*, *11*(3), 201–212. https://doi.org/10.1038/nri2938

Kaczmarek-Hajek, K., Zhang, J., Kopp, R., Grosche, A., Rissiek, B., Saul, A., Bruzzone, S., Engel, T., Jooss, T., Krautloher, A., Schuster, S., Magnus, T., Stadelmann, C., Sirko, S., Koch-Nolte, F., Eulenburg, V., & Nicke, A. (2018). Re-evaluation of neuronal P2X7 expression using novel mouse models and a P2X7-specific nanobody. *eLife*, *7*. https://doi.org/10.7554/eLife.36217

Krzewski, K., & Coligan, J. E. (2012). Human NK cell lytic granules and regulation of their exocytosis. *Frontiers in Immunology*, *3*, 335.

Kursunel, M. A., & Esendagli, G. (2016). The untold story of IFN-gamma in cancer biology. *Cytokine & Growth Factor Reviews*, *31*, 73–81. https://doi.org/10.1016/j.cytogfr.2016.07.005

Lanier, L. L. (2005). NK cell recognition. *Annual Review of Immunology*, *23*, 225–274. https://doi.org/10.1146/annurev.immunol.23.021704.115526

Lee, H., Da Silva, I. P., Palendira, U., Scolyer, R. A., Long, G. V., & Wilmott, J. S. (2021). Targeting NK cells to enhance melanoma response to immunotherapies. *Cancers (Basel)*, *13*(6). https://doi.org/10.3390/cancers13061363

Lilley, E., Stanford, S. C., Kendall, D. E., Alexander, S. P. H., Cirino, G., Docherty, J. R., George, C. H., Insel, P. A., Izzo, A. A., Ji, Y., Panettieri, R. A., Sobey, C. G., Stefanska, B., Stephens, G., Teixeira, M., & Ahluwalia, A. (2020). ARRIVE 2.0 and the British Journal of Pharmacology: Updated guidance for 2020. *British Journal of Pharmacology*, *177*(16), 3611–3616. https://doi.org/10.1111/bph.15178

Livak, K. J., & Schmittgen, T. D. (2001). Analysis of relative gene expression data using real-time quantitative PCR and the 2(-Delta Delta C [T]) method. *Methods*, *25*(4), 402–408. https://doi.org/10.1006/meth.2001.1262

Masin, M., Young, C., Lim, K., Barnes, S. J., Xu, X. J., Marschall, V., Brutkowski, W., Mooney, E. R., Gorecki, D. C., & Murrell-Lagnado, R. (2012). Expression, assembly and function of novel C-terminal truncated variants of the mouse P2X7 receptor: Re-evaluation of P2X7 knockouts. *British Journal of Pharmacology*, *165*(4), 978–993. https://doi.org/10.1111/j.1476-5381.2011.01624.x

Mishra, A., Behura, A., Kumar, A., Naik, L., Swain, A., Das, M., Sarangi, S. S., Dokania, P., Dirisala, V. R., Bhutia, S. K., & Mishra, A. (2021). P2X7 receptor in multifaceted cellular signalling and its relevance as a potential therapeutic target in different diseases. *European Journal of Pharmacology*, *906*, 174235. https://doi.org/10.1016/j.ejphar.2021.174235

Orange, J. S. (2008). Formation and function of the lytic NK-cell immunological synapse. *Nature Reviews. Immunology*, *8*(9), 713–725. https://doi.org/10.1038/nri2381

Orange, J. S., Harris, K. E., Andzelm, M. M., Valter, M. M., Geha, R. S., & Strominger, J. L. (2003). The mature activating natural killer cell immunologic synapse is formed in distinct stages. *Proceedings of the National Academy of Sciences of the United States of America*, *100*(24), 14151–14156. https://doi.org/10.1073/pnas.1835830100

Pegoraro, A., De Marchi, E., & Adinolfi, E. (2021). P2X7 variants in oncogenesis. *Cell*, *10*(1). https://doi.org/10.3390/cells10010189

Pelegrin, P. (2021). P2X7 receptor and the NLRP3 inflammasome: Partners in crime. *Biochemical Pharmacology*, *187*, 114385. https://doi.org/10.1016/j.bcp.2020.114385

Pellegatti, P., Raffaghello, L., Bianchi, G., Piccardi, F., Pistoia, V., & Di Virgilio, F. (2008). Increased level of extracellular ATP at tumor sites: In vivo imaging with plasma membrane luciferase. *PLoS ONE*, *3*(7), e2599. https://doi.org/10.1371/journal.pone.0002599

Percie du Sert, N., Hurst, V., Ahluwalia, A., Alam, S., Avey, M. T., Baker, M., Browne, W. J., Clark, A., Cuthill, I. C., Dirnagl, U., Emerson, M., Garner, P., Holgate, S. T., Howells, D. W., Karp, N. A., Lazic, S. E., Lidster, K., MacCallum, C. J., Macleod, M., … Würbel, H. (2020). The ARRIVE guidelines 2.0: Updated guidelines for reporting animal research. *British Journal of Pharmacology*, *177*(16), 3617–3624. https://doi.org/10.1111/bph.15193

Peruzzi, G., Femnou, L., Gil-Krzewska, A., Borrego, F., Weck, J., Krzewski, K., & Coligan, J. E. (2013). Membrane-type 6 matrix metalloproteinase regulates the activation-induced downmodulation of CD16 in human primary NK cells. *Journal of Immunology*, *191*(4), 1883–1894. https://doi.org/10.4049/jimmunol.1300313

Schmidt, A., Ortaldo, J. R., & Herberman, R. B. (1984). Inhibition of human natural killer cell reactivity by exogenous adenosine 5′-triphosphate. *Journal of Immunology*, *132*(1), 146–150.

Schwarz, E. C., Qu, B., & Hoth, M. (2013). Calcium, cancer and killing: The role of calcium in killing cancer cells by cytotoxic T lymphocytes and natural killer cells. *Biochimica et Biophysica Acta*, *1833*(7), 1603–1611. https://doi.org/10.1016/j.bbamcr.2012.11.016

Senovilla, L., Vacchelli, E., Galon, J., Adjemian, S., Eggermont, A., Fridman, W. H., Sautès-Fridman, C., Ma, Y., Tartour, E., Zitvogel, L., Kroemer, G., & Galluzzi, L. (2012). Trial watch: Prognostic and predictive value of the immune infiltrate in cancer. *Oncoimmunology*, *1*(8), 1323–1343. https://doi.org/10.4161/onci.22009

Sim, G. C., Liu, C., Wang, E., Liu, H., Creasy, C., Dai, Z., Overwijk, W. W., Roszik, J., Marincola, F., Hwu, P., Grimm, E., & Radvanyi, L. (2016). IL2 variant circumvents ICOS+ regulatory T-cell expansion and promotes NK cell activation. *Cancer Immunology Research*, *4*(11), 983–994. https://doi.org/10.1158/2326-6066.CIR-15-0195

Sivori, S., Pende, D., Quatrini, L., Pietra, G., Della Chiesa, M., Vacca, P., Tumino, N., Moretta, F., Mingari, M. C., Locatelli, F., & Moretta, L. (2021). NK cells and ILCs in tumor immunotherapy. *Molecular Aspects of Medicine*, *80*, 100870. https://doi.org/10.1016/j.mam.2020.100870

Sluyter, R. (2017). The P2X7 receptor. *Advances in Experimental Medicine and Biology*, *1051*, 17–53. https://doi.org/10.1007/5584_2017_59

Stabile, H., Fionda, C., Gismondi, A., & Santoni, A. (2017). Role of distinct natural killer cell subsets in anticancer response. *Frontiers in Immunology*, *8*, 293.

Surprenant, A., & North, R. A. (2009). Signaling at purinergic P2X receptors. *Annual Review of Physiology*, *71*, 333–359. https://doi.org/10.1146/annurev.physiol.70.113006.100630

Surprenant, A., Rassendren, F., Kawashima, E., North, R. A., & Buell, G. (1996). The cytolytic P2Z receptor for extracellular ATP identified as a P2X receptor (P2X7). *Science*, *272*(5262), 735–738. https://doi.org/10.1126/science.272.5262.735

Taylor, S. R., Gonzalez-Begne, M., Sojka, D. K., Richardson, J. C., Sheardown, S. A., Harrison, S. M., Pusey, C. D., Tam, F. W., &

Elliott, J. I. (2009). Lymphocytes from P2X7-deficient mice exhibit enhanced P2X7 responses. *Journal of Leukocyte Biology*, *85*(6), 978–986. https://doi.org/10.1189/jlb.0408251

Tremblay-McLean, A., Coenraads, S., Kiani, Z., Dupuy, F. P., & Bernard, N. F. (2019). Expression of ligands for activating natural killer cell receptors on cell lines commonly used to assess natural killer cell function. *BMC Immunology*, *20*(1), 8. https://doi.org/10.1186/s12865-018-0272-x

van Vliet, A. A., Georgoudaki, A. M., Raimo, M., de Gruijl, T. D., & Spanholtz, J. (2021). Adoptive NK cell therapy: A promising treatment Prospect for metastatic melanoma. *Cancers (Basel)*, *13*(18). https://doi.org/10.3390/cancers13184722

Vivier, E., Tomasello, E., Baratin, M., Walzer, T., & Ugolini, S. (2008). Functions of natural killer cells. *Nature Immunology*, *9*(5), 503–510. https://doi.org/10.1038/ni1582

Volonte, C., Apolloni, S., Skaper, S. D., & Burnstock, G. (2012). P2X7 receptors: Channels, pores and more. *CNS & Neurological Disorders Drug Targets*, *11*(6), 705–721. https://doi.org/10.2174/187152712803581137

Watzl, C., & Long, E. O. (2010). Signal transduction during activation and inhibition of natural killer cells. *Current Protocols in Immunology*, *90*, 19B.

Wu, J., Mishra, H. K., & Walcheck, B. (2019). Role of ADAM17 as a regulatory checkpoint of CD16A in NK cells and as a potential target for cancer immunotherapy. *Journal of Leukocyte Biology*, *105*(6), 1297–1303. https://doi.org/10.1002/JLB.2MR1218-501R

Xie, G., Dong, H., Liang, Y., Ham, J. D., Rizwan, R., & Chen, J. (2020). CAR-NK cells: A promising cellular immunotherapy for cancer. *eBioMedicine*, *59*, 102975. https://doi.org/10.1016/j.ebiom.2020.102975

Yan, J., Li, X. Y., Roman Aguilera, A., Xiao, C., Jacoberger-Foissac, C., Nowlan, B., Robson, S. C., Beers, C., Moesta, A. K., Geetha, N., Teng, M. W. L., & Smyth, M. J. (2020). Control of metastases via myeloid CD39 and NK cell effector function. *Cancer Immunology Research*, *8*(3), 356–367. https://doi.org/10.1158/2326-6066.CIR-19-0749

Young, C. N. J., & Gorecki, D. C. (2018). P2RX7 Purinoceptor as a therapeutic target-the second coming? *Frontiers in Chemistry*, *6*, 248. https://doi.org/10.3389/fchem.2018.00248

Zhou, X., Friedmann, K. S., Lyrmann, H., Zhou, Y., Schoppmeyer, R., Knorck, A., Mang, S., Hoxha, C., Angenendt, A., Backes, C. S., & Mangerich, C. (2018). A calcium optimum for cytotoxic T lymphocyte and natural killer cell cytotoxicity. *The Journal of Physiology*, *596*(14), 2681–2698. https://doi.org/10.1113/JP274964

Zingoni, A., Vulpis, E., Loconte, L., & Santoni, A. (2020). NKG2D ligand shedding in response to stress: Role of ADAM10. *Frontiers in Immunology*, *11*, 447. https://doi.org/10.3389/fimmu.2020.00447

Zloza, A., Dharmadhikari, N. D., Huelsmann, E. J., Broucek, J. R., Hughes, T., Kohlhapp, F. J., & Kaufman, H. L. (2017). Low-dose interleukin-2 impairs host anti-tumor immunity and inhibits therapeutic responses in a mouse model of melanoma. *Cancer Immunology, Immunotherapy*, *66*(1), 9–16. https://doi.org/10.1007/s00262-016-1916-4

SUPPORTING INFORMATION

Additional supporting information can be found online in the Supporting Information section at the end of this article.

How to cite this article: Baroja-Mazo, A., Peñín-Franch, A., Lucas-Ruiz, F., de Torre-Minguela, C., Alarcón-Vila, C., Hernández-Caselles, T., & Pelegrín, P. (2022). P2X7 receptor activation impairs antitumour activity of natural killer cells. *British Journal of Pharmacology*, 1–18. https://doi.org/10.1111/bph.15951